Doctoral Dissertation

Structural Control of Metal-Metal Interaction in Bioorganometallic Compounds Bearing Uracil Moieties

Yuki Sakamoto

April 2015

Department of Applied Chemistry

Graduate School of Engineering,

Osaka University

Structural Control of Metal-Metal Interaction in Bioorganometallic Compounds Bearing Uracil Moieties

（ウラシル部位を有する生物有機金属化合物における
金属間相互作用の構造的制御）

2015

Yuki Sakamoto

Department of Applied Chemistry
Graduate School of Engineering,
Osaka University

Preface

The studies presented in this thesis were performed under the guidance of Professor Toshikazu Hirao, Department of Applied Chemistry, Graduate School of Engineering, Osaka University during 2009-2015.

The objects of this thesis are studies on controlling the metal-metal interaction of bioorganometallic compounds bearing uracil moieties as nucleobases.

The author hopes that this basic work described in this thesis contributes to the further development of bioorganometallic compounds, structural control of organometallic complexes, and so on.

Yuki Sakamoto

Department of Applied Chemistry

Graduate School of Engineering

Osaka University

Suita, Osaka

Japan

April, 2015

Contents

General Introduction

The structural control of molecular self-organization leads to the development of functional materials.[1] Non-covalent bond is useful for the formation of self-assembling structures. Control of hydrogen bonding[2] plays an important role in the design of diverse molecular assemblies because of its directionality and specificity.[3] Reversibility and tuneability of hydrogen bonding are also significant to affect the chemical and/or physical properties of molecular assemblies.

On the other hand, highly organized molecular aggregates are constructed in biosystems to accomplish unique functions as shown in enzymes, receptors, etc. Biomolecules such as nucleobases, peptides, and sugars play an important role in the formation of the highly organized structures like DNA, proteins, and enzymes. For example, the double helical DNA is composed of adenine-thymine and guanine-cytosine base pairs, which are managed mainly by complementary hydrogen bondings, π-π interactions, and hydrophobic interactions.[4] Nucleobases possess a particular ability to perform directionally controlled multiple and complementary hydrogen bondings. The utilization of nucleobases in bio-inspired systems provides the flexibility to exploit four different binding motifs. The employment of self-assembling properties of nucleobases is considered to be an appropriate strategy for a design of well-defined molecular aggregates.[5]

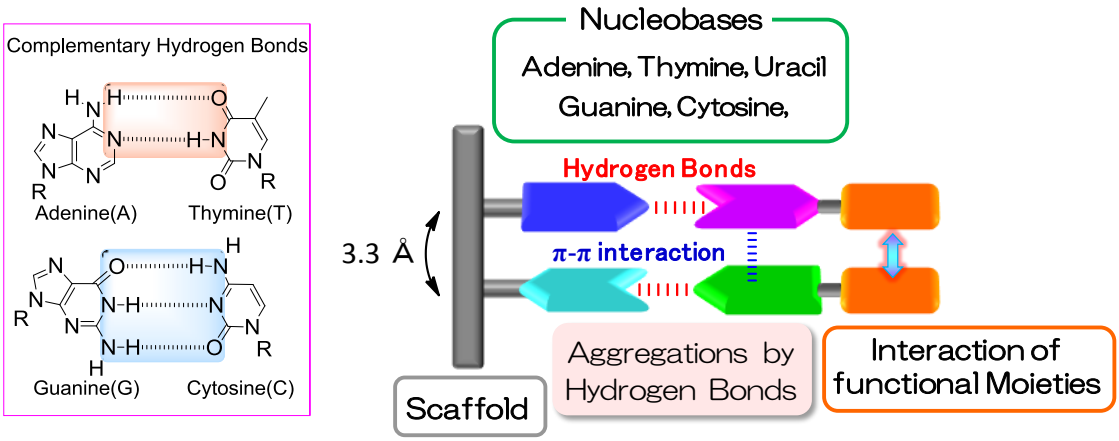

Figure 1. Watson-Crick-like nucleobase pairing and an aggregation system by using nucleobases

Uracil is one of major nucleobases and used in RNA instead of thymine in DNA. Uracil consists of pyrimidine ring and possesses alternately adjacent two hydrogen bond donors (D) and two hydrogen bond acceptors (A) (Figure 2). Owing to the order of acceptor-donor-acceptor (ADA) of hydrogen bonds, uracil can form three hydrogen bonds with DAD-typed hydrogen bonding sites. 2,6-diamidopyridine derivatives which have DAD-typed hydrogen bonding sites are adopted as the complementary hydrogen bonding moieties for uracil in construction of organized-assembling structures by using of uracil. For example, Lehn's group reported formation of supramolecular liquid crystalline polymers through the complementary three hydrogen bonds between uracil with a 2,6-diamidopyridine derivative (Figure 3a).[6] Inouye's group also published molecular recognition of thymine by using a scaffold bearing a 2,6-diamidopyridine derivative and a π–conjugate compound (Figure 3b).[7] A functional moiety can also be introduced to uracil in both fifth and sixth positions of the pyrimidine ring unlike

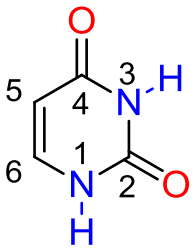

Figure 2. Structure of uracil

thymine. Orientation of hydrogen bonds for the functional moiety can be regulated by the position of introduction. The above mentioned properties of uracil are useful for controlled arrangement of the functioned moieties.

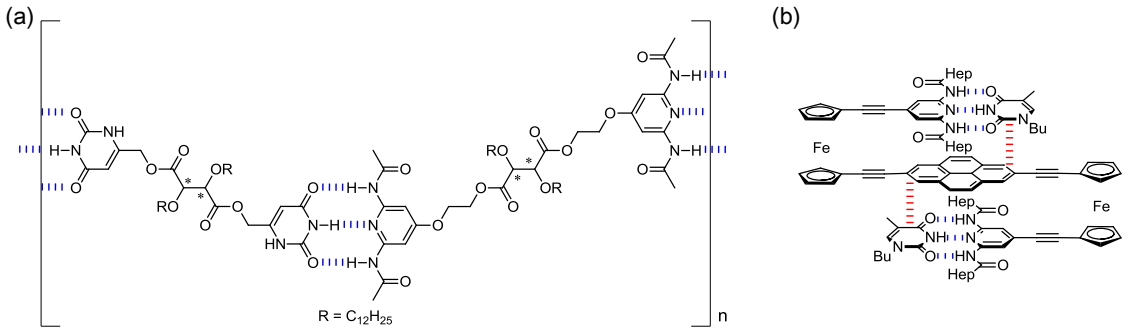

Figure 3. (a) Supramolecular liquid crystalline polymers and (b) molecular recognition of a thymine derivative by using a scaffold through the complementary hydrogen bonds.

Organometallic compounds have attracted much attention in not only synthetic organic chemistry but materials science because of utility of photochemical and catalytic abilities and redox properties. The control of the structural properties of metal centers is significant to manage the functions of the complexes. It is known that metal-metal interaction in the organometallic compounds affects the functions of the complexes as catalysis, emission property etc. In particular, square-planar d^8 transition metals and linear geometric d^{10} transition metals exhibit a unique emission and catalytic properties based on induced metal-metal interaction owing to stacking of planar or linear complexes. However, it is a problem that a multi-step synthesis is necessary for an organometallic complex induced the metal-metal interaction.

Square-planar d^8 transition metal complexes have intriguing photochemical properties. In particular, platinum(II) complexes with oligopyridine or cyclometalating ligands have drawn much attention due to their interesting luminescence properties based on Pt(II)–Pt(II) interaction.[8] Emission properties of phenylbipyridine type platinum(II) complexes were reported to be changed by the Pt(II)-Pt(II) interaction (Figure 4). For instance, Wai-Yeung Wong and co-workers have published the change of emission properties through the control of a distance of two platinum(II) moieties based on electrostatic interaction between the ligands (Scheme 1a).[9] Hirao's group has also reported the switching of emission properties based on conformational change of the dinuclear platinum(II) complex depending on the solvent polarity(Scheme 1b).[10]

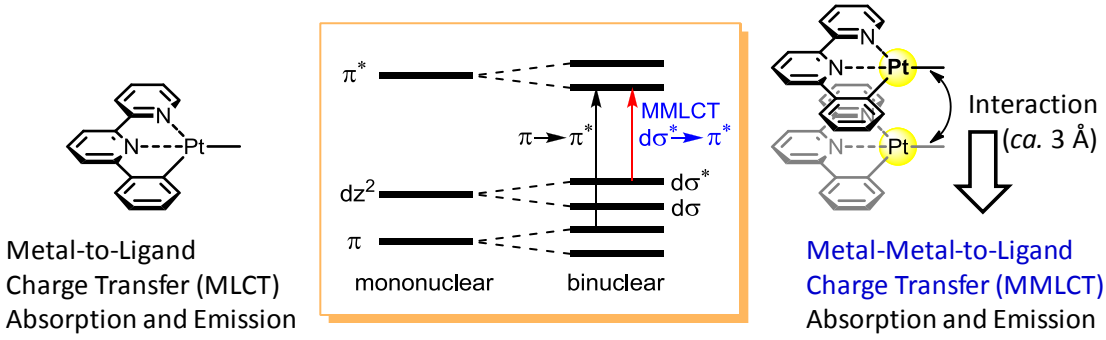

Figure 4. Diagrams of metal-metal-to-ligand charge transfer through Pt(II)–Pt(II) interaction of phenylbipyridine-typed platinum(II) complexes

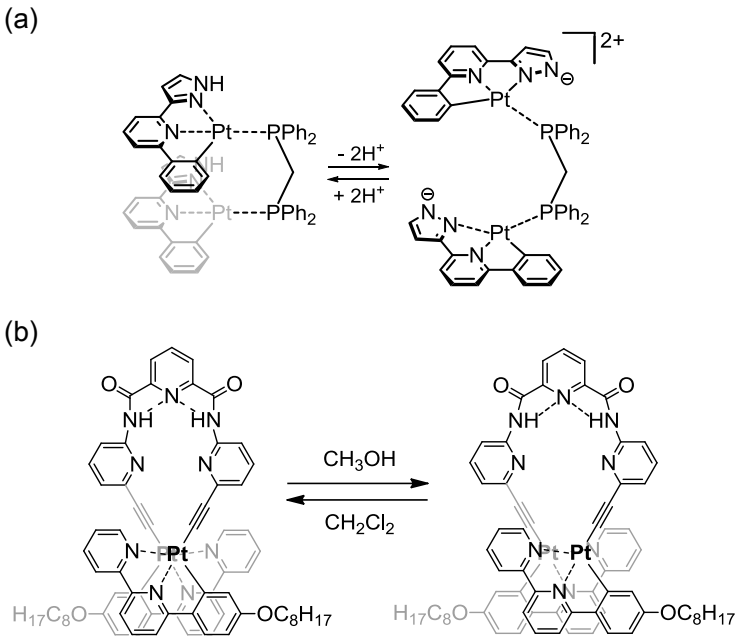

Scheme 1.

A organogold(I) complex, which is a linear geometric d^{10} transition metal, has drawn increasing attention because of aggregation properties through attractive aurophilic interaction.[11] This aurophilic interaction is comparable to the strength of hydrogen bonding and convenient for construction of supramolecular architectures in a solid state (Figure 5). Gold(I) alkynyl compounds have also attracted attention in a variety of areas due to their diverse and interesting photophysical[12] and biological[13] properties. In 1993, Shie-Ming Peng and co-workers reported the emission of a gold(I) alkynyl compound based on Au(I)-Au(I) interaction in a solid state.[12a]

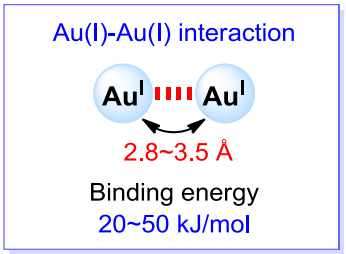

Figure 5. Diagram of Au(I)-Au(I) interaction

The introduction of functional complexes into highly-ordered biomolecules is considered to be a convenient approach to design novel biomaterials and bio-inspired systems. Recently, the research field of bioorganometallic chemistry, which is a hybrid area between organometallic chemistry and biochemistry, has received extensive interest.[14] The combination of functional organometallic compounds with biomolecules such as nucleobases and peptides is envisioned to afford bioorganometallic compounds. The bioorganometallic compounds are expected to be applicated for probes, catalysts and medicines owing to synergistic effect of both properties of organometallic compounds and biomolecules. For example, Richard H. Fish and co-workers, Gérard Jaouen and co-workers, and Gerard van Koten and co-workers reported the synthesis of a rhodium complex bearing guanosine,[15] a chromium complex bearing an estradiol derivative,[16] and a platinum complex bearing valine[17] respectively (Figure 6a-c). Hirao's group has also published the formation of a chiral organized structure of ferrocene bearing dipeptides through intermolecular hydrogen bonds of the dipeptides (Figure 6d).[18]

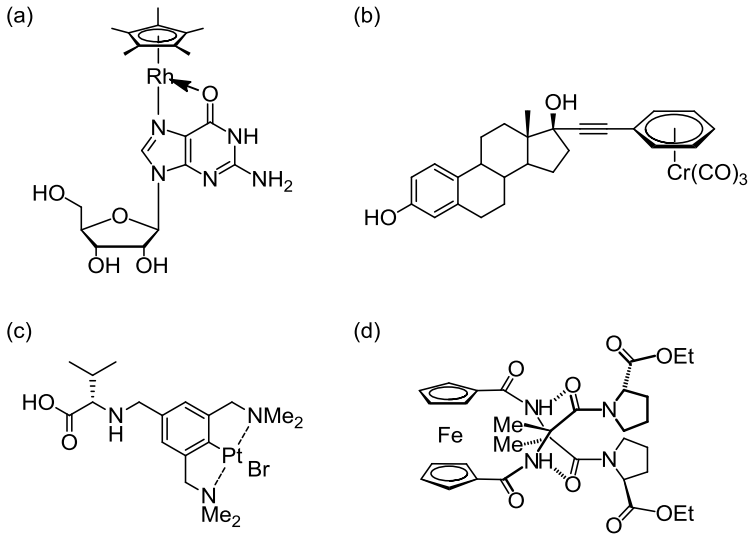

Figure 6. Bioorganometallic compounds composed of organometallic and biomolecular moieties such as nucleobase, amino acid and peptide.

From these points of view, a combination of organoplatinum(II) and gold(I) complexes with uracils as nucleobases is allowed to design novel bioconjugates and controlled arrangement of metal centers depending on both properties. Uracil is useful for the construction of supramolecular systems due to its hydrogen bonding capacity, which forms complementary hydrogen bonds for 2,6-diamidopyridine derivatives. Arrangement of the metal centers by application of assembly property of the uracils is convenient for induction of the metal-metal interaction. On the other hand, ancillary ligands of the complexes play an important role in aggregation of metal centers. Steric hinderance and π–π interaction of the ancillary ligands affect the assembly properties of the organometal-uracil conjugates.

The dissertation deals with studies on syntheses of organoplatinum(II) and organogold(I) complexes bearing the uracil moieties and structural control of metal-metal interaction through molecular scaffolds and ancillary ligands.

Chapter 1 describes synthesis of organoplatinum(II)-uracil conjugates and controlled arrangement of the platinum(II)complexes by using molecular scaffolds.

Chapter 2 describes syntheses of organogold(I)-uracil conjugates and evaluation of steric effect of ancillary ligands for assembly properties of the gold(I) centers.

Chapter 3 describes syntheses of dinuclear organogold(I)-uracil conjugates with bridging diphosphine ligands and induced Au(I)-Au(I) interaction.

References

1. (a) D. Braga, F. Grepioni and G.R. Desiraju, *Chem. Rev.* 1998, **98**, 1375; (b) V. Balzani, A. Credi, F.M. Raymo and J.F. Stoddart, *Angew. Chem. Int. Ed.* 2000, **39**, 3348; (c) G.F. Swiegers and T.J. Malefetse, *Chem. Rev.* 2000, **100**, 3483.
2. G. A. Jeffrey, *An introduction to hydrogen bonding*, 1st ed. Oxford University Press, New York, 1997
3. (a) M. M. Conn and J. Rebek, Jr., *Chem. Rev.*, 1997, **97**, 1647; (b) E. A. Archer, H. Gong and M. J. Krische, *Tetrahedron*, 2001, **57**, 1139; (c) L. J. Prins, D. N. Reinhoudt and P. Timmerman, *Angew. Chem. Int. Ed.*, 2001, **40**, 2382.
4. W. Saenger, Principles of Nucleic Acid Structure, Springer-Verlag, New York, 1984.
5. For recent reviews, see: (a) S.Sivakova and S.J.Rowan, *Chem. Soc. Rev.* 2005, **34**, 9; (b) J.T. Davis and G.P. Spada, *Chem. Soc. Rev.* 2007, **36**, 296; (c) J.L. Sessler, C.M. Lawrence and J. Jayawickramarajah, *Chem. Soc. Rev.* 2007, **36**, 314; (d) K. Tanaka and M. Shionoya, *Coord. Chem. Rev.* 2007, **251**, 2732; (e) J. Müller, *Eur. J. Inorg. Chem.* 2008, 3749; (f) S. Lena, S.Masiero, S. Pieraccini and G.P. Spada, *Chem. Eur. J.* 2009, **15,** 7792; (g) G.H. Clever and M. Shionoya, *Coord. Chem. Rev.* 2010, **254**, 2391.
6. C. Fouquey, J.-M. Lehn and A. M. Levelut, *Adv. Mater.* 1990, **2**, 254.
7. M. Inouye, M. S. Itoh, and H. Nakazumi, J. Org. Chem. 1999, **64**, 9393.
8. For recent reviews, see: (a) D. M. Roundhill, H. B. Gray and C.-M. Che, *Acc. Chem. Res.*, 1989, **22**, 55; (b) V. H. Houlding and V. M. Miskowski, *Coord. Chem. Rev.*, 1991, **111**, 145; (c) M. Kato, *Bull. Chem. Soc. Jpn.*, 2007, **80**, 287; (d) I. Eryazici, C. N. Moorefield and G. R. Newkome, *Chem. Rev.*, 2008, **108**, 1834; (e) J. A. G. Williams, S. Develay, D. L. Rochester and L. Murphy, *Coord. Chem. Rev.*, 2008, **252**, 2596; (f) R. McGuire Jr., M. C. McGuire and D. R. McMillin, *Coord. Chem. Rev.*, 2010, **254**, 2574; (g) K. M.-C. Wong and V. W.-W. Yam, *Acc. Chem. Res.*, 2011, **44**, 424.
9. C.-K.Koo, B. Lam, S.-K. Leung, H.-W. M. Lam and W.-Y. Wong, *J. Am. Chem. Soc.* 2006, **128**, 16435.
10. A. Gross, T. Moriuchi and T. Hirao, *Chem. Commun.* 2013, **49**, 1163.
11. For recent reviews, see: (a) H. Schmidbaur, *Chem. Soc. Rev.* 1995, **24** 391; (b) P. Pyykkő, *Chem. Rev.* 1997, **97**, 597; (c) M. J. Katz, K. Sakai and D. B. Leznoff, *Chem. Soc. Rev.* 2008, **37**, 1884; (d) I. Ott, *Coord. Chem. Rev.* 2009, **253,** 1670; (e) H. Schmidbaur and A. Schier, *Chem. Soc. Rev.* 2012, **41**, 370.

12. (a) D. Li, X. Hong, C. M. Che, W. C. Lo and S. M. Peng, *J. Chem. Soc. Dalton Trans.* 1993, 2929; (b) H. Xiao, Y. X. Weng, S. M. Peng and C. M. Che, *J. Chem. Soc. Dalton Trans.* 1996, 3155; (c) M. J. Irwin, J. J. Vittal and R. J. Puddephatt, *Organometallics* 1997, **16**, 3541; (d) C. M. Che, H. Y. Chan, V. M. Miskowski, Y. Li and K. K. Cheung, *J. Am. Chem. Soc.* 2001, **123**, 4985.
13. (a) E. Schuh, S. M. Valiahdi, M. A. Jakupec, B. K. Keppler, P. Chiba and F. Mohr, *Dalton Trans.* 2009, 10841; (b) E. Vergara, E. Cerrada, A. Casini, O. Zava, M. Laguna and P. J. Dyson, *Organometallics* 2010, **29**, 2596; (c) A. Meyer, C. P. Bagowski, M. Kokoschka, M. Stefanopoulou, H. Alborzinia, S. Can, D. H. Vlecken, W. S. Sheldrick, S. Wölfl and I. Ott, *Angew. Chem. Int. Ed.* 2012, **51**, 8895; (d) A. Meyer, A. Gutiérrez, I. Ott and L. Rodríguez, *Inorg. Chim. Acta* 2013, **398**, 72.
14. (a) G. Jaouen, A. Vessiéres and I. S. Butler, *Acc. Chem. Res.* 1993, **26**, 361; (b) R. Severin, R. Bergs and W. Beck, *Angew. Chem. Int. Ed.* 1998, **37**, 1634; (c) R. H. Fish and G. Jaouen, *Organometallics* 2003, **22**, 2166; (d) T. Moriuchi and T. Hirao, *Chem. Soc. Rev.* 2004, **33**, 294; (e) D. R. van Staveren and N. Metzler-Nolte, *Chem. Rev.* 2004, **104**, 5931; (f) H. Song, X. Li, Y. Long, G. Schatte and H.-B. Kraatz, *Dalton Trans.* 2006, 4696; (g) W. Beck, *Z. Naturforsch. B* 2009, **64**, 1221; (h) A. Lataifeh, S. Beheshti and H.-B. Kraatz, *Eur. J. Inorg. Chem.* 2009, 3205; (i) T. Moriuchi and T. Hirao, *Acc. Chem. Res.* 2010, **43**, 1040; (j) G. Gasser, A. M. Sosniak and N. Metzler-Nolte, *Dalton Trans.* 2011, **40**, 7061; (k) B. Adhikari, R. Afrasiabi and H.-B. Kraatz, *Organometallics* 2013, **32**, 5899.
15. D. P. Smith, E. Baralt, B. Morales, M. M. Olmstead, M. F. Maestre and R. H. Fish, *J. Am. Chem. Soc.* 1992, **114**, 10647.
16. H. E. Amouri, A. Vessieres, D. Vichard, S. Top, M. Gruselle and G. Jaouen, *J. Med. Chem.* 1992, **35**, 3130.
17. G. Guillena, G. Rodríguez and G. van Koten, *Tetrahedron Lett.* 2002, **43**, 3895.
18. A. Nomoto, T. Moriuchi, S. Yamazaki, A. Ogawa and T. Hirao, *Chem. Commun.* 1998, 1963.

Chapter 1. Controlled arrangement of organoplatinum(II) complexes bearing uracil moieties by using molecular scaffolds

1-1. Introduction

As mentioned in general introduction, square-planar d^8 transition metal complexes possess the intriguing photophysical and photochemical properties. In particular, luminescent platinum(II) complexes with oligopyridine and cyclometalating ligands have attracted much attention. It is reported that the luminescent platinum(II) complexes with a phenylbipyridine ligand exhibited an interesting luminescence properties based on metallophilic interaction through $d_Z^2 \bullet\bullet\bullet d_Z^2$ and/or π-π interactions.[1] On the other hands, uracil is useful for construct of supramolecular systems due to its hydrogen bonding capacity. Uracil formed a complementary hydrogen bonds for 2,6-diamidopyridine derivatives and have two position for introduction of a functional moiety.[2] From these points of view, I report the syntheses of the bioorganometallic compounds by conjugation of the uracils and the organoplatinum(II) compounds and controlled emission properties based on the regulation of aggregation of platinum(II) centers in the chapter 1 (Figure 1).

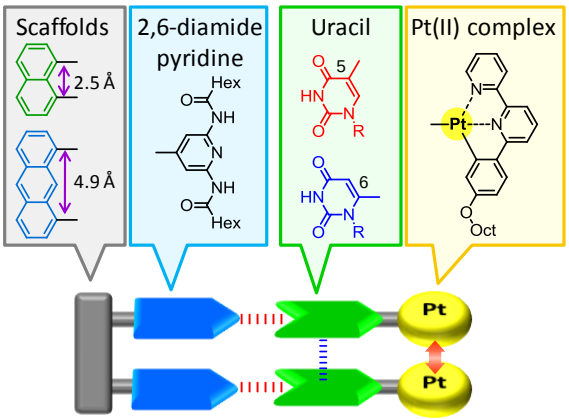

Figure 1. Design of the bioorganometallic compounds composed of uracils and organoplatinum(II) complexes, and molecular scaffolds.

1-2. Results and discussion

1-2-1. Syntheses and structural properties of organoplatinum(II) complexes bearing uracil moieties

The bioorganometallic platinum(II) compounds **U6Pt** and **U5Pt** were obtained by the treatment of [4-octyloxy-(C^N^N)PtCl] (**2**), which was prepared from the reaction of 6-(4-octyloxyphenyl)-2,2'-bipyridine (**1**) and K_2PtCl_4, with 6-ethynyl-1-octyluracil or 5-ethynyl-1-octyluracil, respectively (Scheme 1).

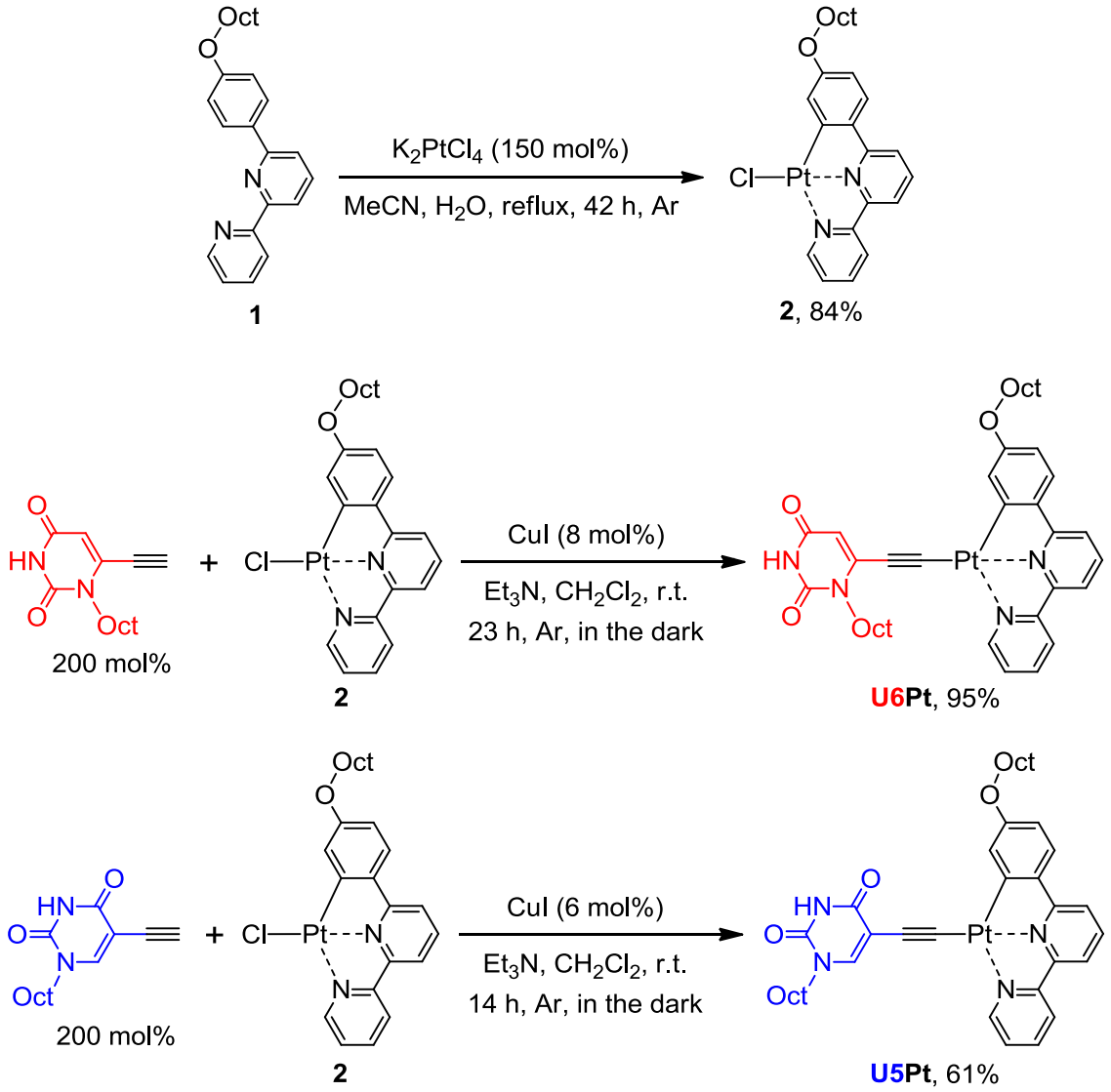

Scheme 1.

Structural information was found by a single-crystal X-ray structure determination. The formation of the dimeric structure through intermolecular hydrogen bonds between the uracil moieties of two independent molecules was exhibited in the crystal structure of **U6Pt** (Figure 2a and Table 1). The [4-octyloxy-(C^N^N)Pt] moiety is nearly parallel to the uracil moiety probably due to the d,π-conjugation; the dihedral angles between the least squares plane of the [4-octyloxy-(C^N^N)Pt] and the uracil moieties are 19.8(3) and 14.8(3)°. Furthermore, a packing structure of **U6Pt** revealed that each hydrogen-bonded dimer were connected through π-π interactions between the [4-octyloxy-(C^N^N)Pt] ligands as well as uracil moieties to form π-stacks. Pt(II)-Pt(II) interaction (the intermolecular Pt-Pt distance is ca. 3.3 Å) was observed, as shown in Figure 2b.

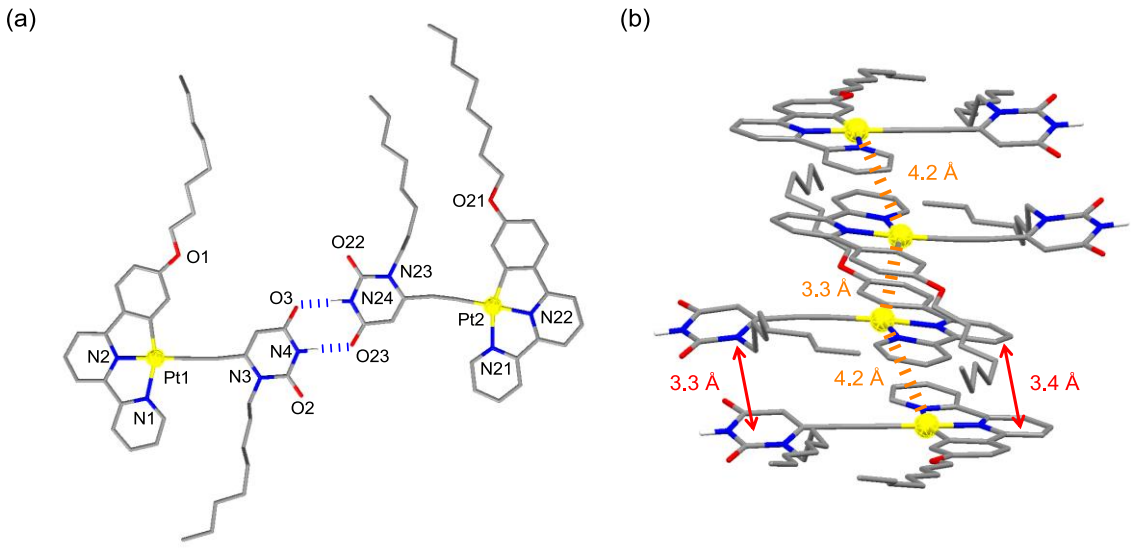

Figure 2. (a) A dimer structure of **U6Pt** through intermolecular hydrogen bonds between the uracil moieties and (b) a portion of a packing structure of **U6Pt** layer containing the π-stack molecular assembly through π-π interactions between the [4-octyloxy-(C^N^N)Pt] ligands as well as uracil moieties.

Table 1. Intermolecular hydrogen bonds for **U6Pt**[a]

Donor	Acceptor	D•••A (Å)	D–H•••A (°)
N(4)	O(23)[b]	2.787(10)	175(5)
N(24)[b]	O(3)	2.819(10)	170(4)
N(24)	O(3)[b]	2.819(10)	170(4)
N(4)[b]	O(23)	2.787(10)	175(5)

(a) Two independent molecules exist in an asymmetric unit.

(b) –X+2, –Y+1, –Z+1.

This π-π and Pt(II)-Pt(II) interactions might require the orientation of the [4-octyloxy-(C^N^N)Pt] moiety within a limited range of location parallel to the uracil moiety. In fact, the platinum(II) complex **U6Pt** showed the emission band around 720 nm, ascribed to the triplet metal-metal-to-ligand charge transfer (^{3}MMLCT) excited state resulting from Pt(II)-Pt(II) and π-π interactions, in a solid state (Figure 3). In contrast, the platinum(II) complex **U5Pt**, wherein the direction of hydrogen bonding sites of the uracil moieties is different from **U6Pt**, exhibited an emission band based on the metal-to-ligand charge transfer (MLCT) and/or ligand-to-ligand charge transfer (LLCT) transition. Synergistic effects of emission properties are considered to depend on the aggregation properties of the platinum(II) complexes.

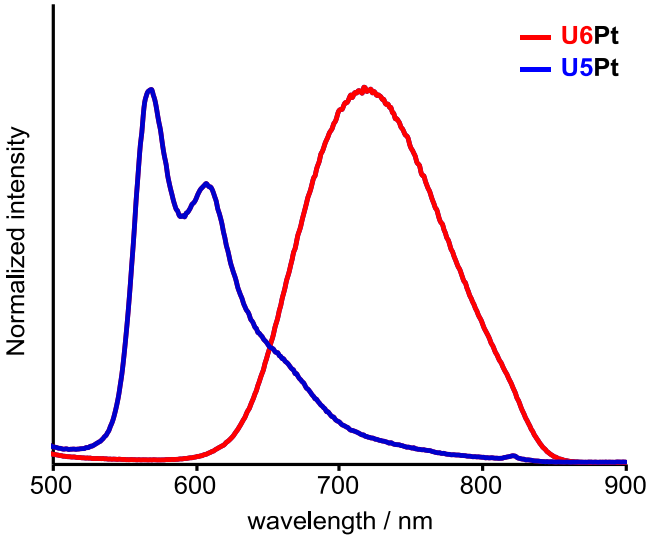

Figure 3. Emission spectra (λ_{ex} = 470 nm) of **U6Pt** and **U5Pt** in solid states at 298 K.

1-2-2. Controlled arrangement of organoplatinum(II) complexes bearing uracil moieties by using molecular scaffolds

To control the aggregate of the organoplatinum(II) complexes having uracil moieties, molecular scaffolds **ND** and **AD** combined aromatic rigid frameworks, naphthalene and anthracene, respectively, with two 2,6-dihexamidopyridine moieties as a complementary hydrogen bonding site for the uracil moiety were designed and synthesized as shown in Schemes 2 and 3. The coupling reaction of 1,8-diiodonaphthalene with 2,6-dihexamido-4-ethynylpyridine (**7**) afforded the molecular scaffold **ND** by using the palladium-catalyzed Sonogashira coupling procedure in 40% yield. The molecular scaffold **AD** was prepared by the coupling reaction of 1,8-diethynylanthracene and 4-(2,6-dihexamidopyridyl) trifluoromethanesulfonate (**5**) in 28% yield.

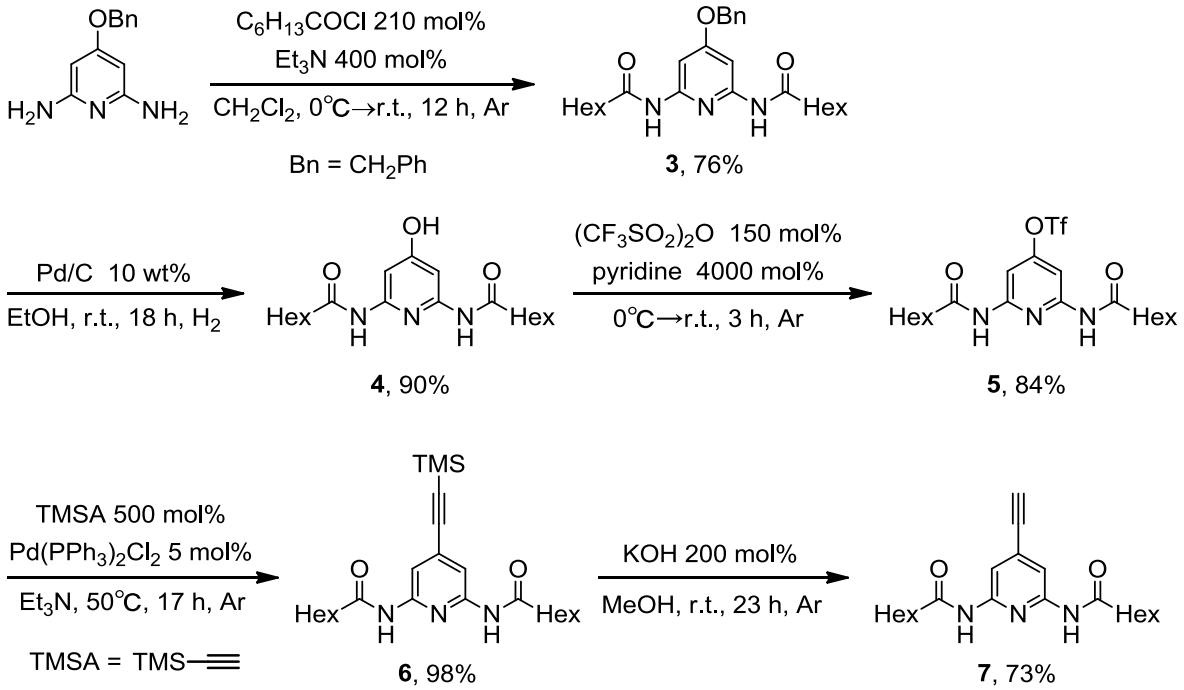

Scheme 2.

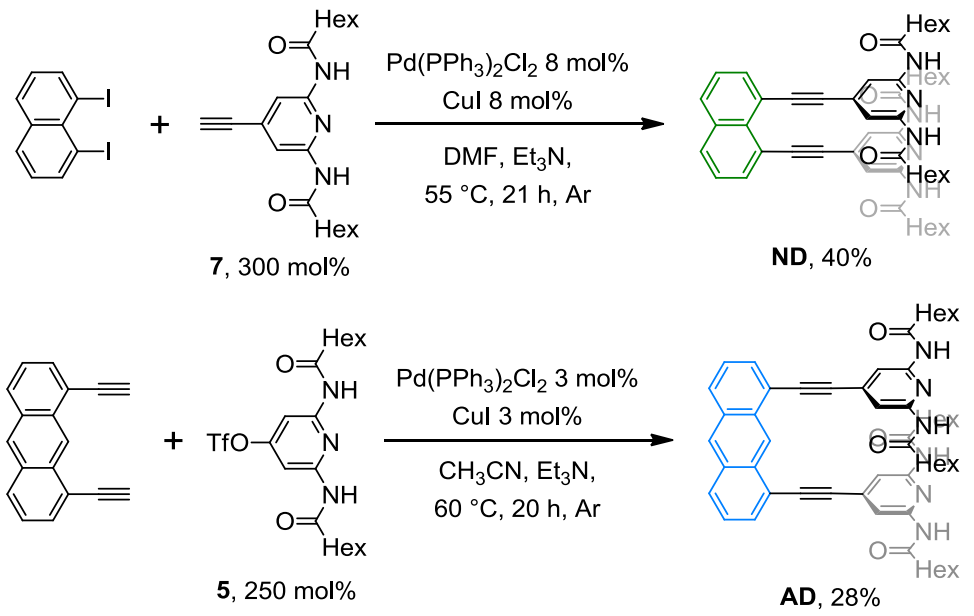

Scheme 3.

In a case of addition of 0.5 molar equiv. amounts of **ND** to a dichloromethane solution of **U6Pt**, a new shoulder band at around 500 nm was found in the UV/vis spectrum as shown in Figure 4a. The absorption at around 500 nm is probably attributed to the MMLCT transition based on the aggregation of **U6Pt** through the complementary hydrogen bondings to **ND**. The emission spectrum of only **U6Pt** in dichloromethane exhibited emission band at 590 nm, which is assigned to a ^{3}MLCT and/or ^{3}LLCT emission (Figure 4b). Interestingly, **U6Pt** showed a new emission band based on synergistic effect around 730 nm with decrease of the ^{3}MLCT/^{3}LLCT emission in the presence of the molecular scaffold **ND** (Figure 4b). This emission band is assignable to a ^{3}MMLCT emission based on Pt(II)-Pt(II) and π-π interactions between the [4-octyloxy-(C^N^N)Pt] and uracil moieties as shown in Figure 4b. The molecular scaffold **ND** was found to facilitate aggregation of **U6Pt** through the complementary hydrogen bonding and π-π interaction between the ligands in a solution state. The 1:2 stoichiometry of **ND**-**U6Pt** was verified by Job's plots. The stepwise association constants (K_1 and K_2 in M^{-1}) were evaluated to be logK_1 = 3.7(3) and logK_2 = 4.1(2), respectively, for 1:2 complexation of **ND** with **U6Pt**.[3] The value for the ratio $4K_2/K_1$ = ~16 clearly indicates the positive homotropic cooperative nature of this complexation.

The metallophilic and π-π interactions are likely to induce the positive cooperative effect. In the case of using **U5Pt**, such absorption and emission resulting from Pt(II)-Pt(II) and π-π interactions were hardly observed (Figures 5a and 5b) although 1:2 complexation of **ND** with **U5Pt** was verified by Job's plots. The decrease in K values (logK_1 = 2.95(2) and logK_2 = 2.82(9)) between **ND** and **U5Pt** was observed.[3] These results indicate the importance of the direction of the hydrogen bonding sites to arrange the [4-octyloxy-(C^N^N)Pt] moieties regularly.

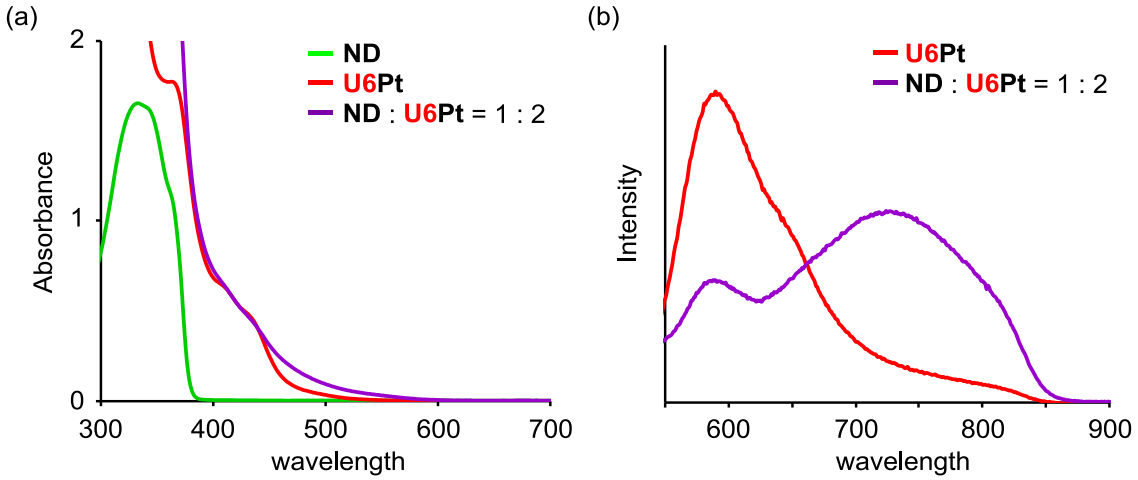

Figure 4. (a) UV/vis spectra of **ND**, **U6Pt**, and **ND-U6Pt** (1:2) in dichloromethane ([**ND**] = 0.5 x 10^{-3} M, [**U6Pt**] = 1.0 x 10^{-3} M) at 298 K, (b) emission spectra (λ_{ex} = 530 nm) of **U6Pt** and **ND-U6Pt** (1:2) in dichloromethane ([**ND**] = 0.5 x 10^{-3} M, [**U6Pt**] = 1.0 x 10^{-3} M) at 298 K,

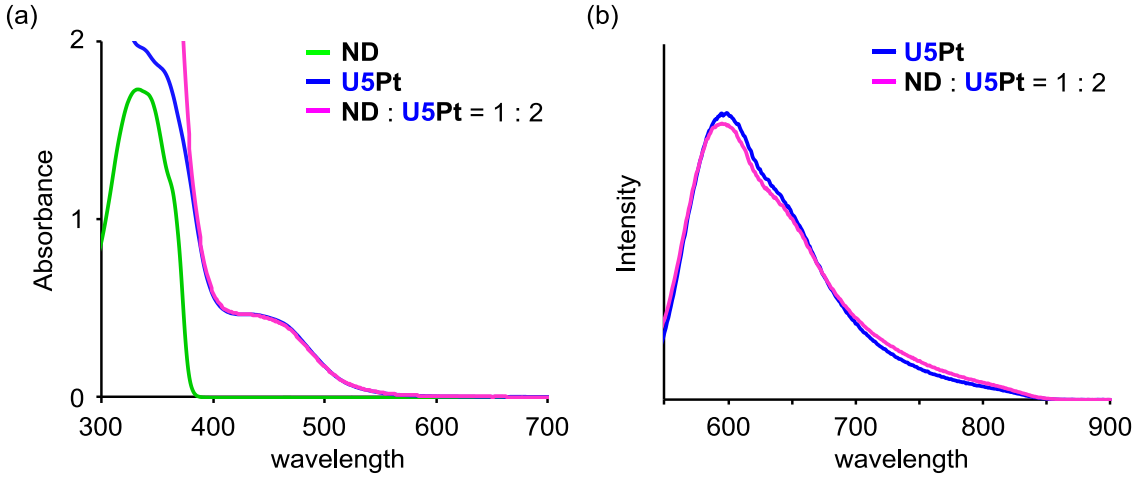

Figure 5. UV/vis spectra of **ND**, **U5Pt**, and **ND-U5Pt** (1:2) in dichloromethane ([**ND**] = 0.5 x 10^{-3} M, [**U5Pt**] = 1.0 x 10^{-3} M) at 298 K, (b) emission spectra (λ_{ex} = 530 nm) of **U5Pt** and **ND-U5Pt** (1:2) in dichloromethane ([**ND**] = 0.5 x 10^{-3} M, [**U5Pt**] = 1.0 x 10^{-3} M) at 298 K.

The Pt(II)-Pt(II) and π-π interactions in aggregated complexes is considered to be influenced by an interbase distance. The change of Pt(II)-Pt(II) and π–π interactions might be reflected on their absorption and emission properties. The molecular scaffold **AD** was also ascertained to form the 1:2 complex with **U6Pt** by Job's plots, wherein the stepwise association constants (K_1 and K_2) were appraised to be logK_1 = 5.05(4) and logK_2 = 4.189(6), respectively.[3] The appearance of a new shoulder band around 500 nm was caused by the addition of 0.5 molar equiv. amounts of **AD** composed of anthracene to a dichloromethane solution of **U6Pt** in the UV/vis spectrum. The new shoulder band is assignable to the MMLCT transition based on Pt(II)-Pt(II) and π-π interactions (Figure 6a). By the addition of 0.5 molar equiv. amounts of **AD**, the increase of the ^{3}MMLCT emission at around 730 nm based on its synergistic effect and the decrease of the ^{3}MLCT/^{3}LLCT emission were also observed in the emission spectrum as shown in Figure 6b.

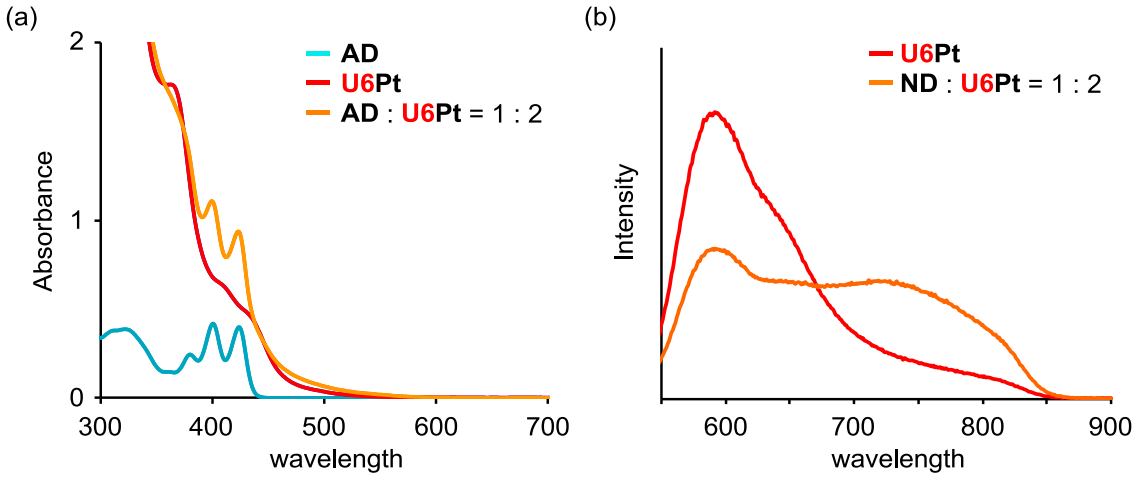

Figure 6. UV/vis spectra of **AD**, **U6Pt**, and **AD-U6Pt** (1:2) in dichloromethane ([**AD**] = 0.5 x 10^{-3} M, [**U6Pt**] = 1.0 x 10^{-3} M) at 298 K, (b) emission spectra (λ_{ex} = 530 nm) of **U6Pt** and **AD-U6Pt** (1:2) in dichloromethane ([**AD**] = 0.5 x 10^{-3} M, [**U6Pt**] = 1.0 x 10^{-3} M) at 298 K.

In comparison to the emission with the molecular scaffold **ND** composed of naphthalene, **U6Pt** aggregates with the **AD** exhibited the low intensity of the ^{3}MMLCT emission and the high intensity of the ^{3}MLCT emission probably because of the weak Pt(II)-Pt(II) and π-π interactions based on the longer interbase distance (Figure 7). The emission properties of **U6Pt** was revealed to be controlled by changing the molecular scaffold size.

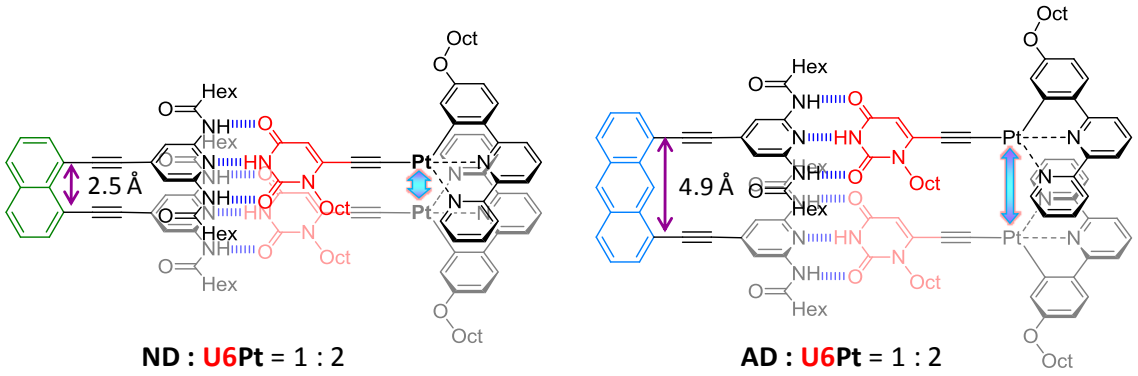

Figure 7. Schematic depiction of the controlled aggregation of the bioorganometallic platinum(II) compound **U6Pt** by using the molecular scaffolds of **ND** and **AD**.

1-3. Conclusion

In conclusion, the designed organoplatinum(II)-uracil conjugate **U6Pt** was performed to form the dimeric structure through intermolecular hydrogen bonds between the uracil moieties of two independent molecules. The each hydrogen-bonded dimer was connected through Pt(II)-Pt(II) and π–π interactions in a packing structure. The tuning of the emission properties of the organoplatinum(II)-uracil conjugates was attained by changing the direction of hydrogen bonding sites and the molecular scaffold size. which affected the regulation of the aggregated structures, to induce the Pt(II)-Pt(II) and π–π interactions. The architectural control of molecular assemblies using preorganized molecular scaffolds is envisaged to be a useful approach to artificial highly-ordered systems without chemical synthesis.

1-4. Experimental section

General methods

All reagents and solvents were purchased from commercial sources and were further purified by the standard methods, if necessary. All manipulations were performed under Ar. Melting points were measured with a Yanagimoto Micromelting Point Apparatus and were uncorrected. Infrared spectra were obtained with a JASCO FT/IR-480 Plus spectrometer. ^{1}H NMR spectra were recorded on a JEOL JNM-ECS 400 (400 MHz) spectrometer with tetramethylsilane as an internal standard. Mass spectra were run on a JEOL JMS DX-303 spectrometer.

6-Ethynyl-1-octyluracil,[4] 5-ethynyl-1-octyluracil,[5] 4-benzyloxy-2,6-pyridinediamine,[6] 1,8-diiodonaphthalene[7] and 1,8-diethynylanthracene[8] were prepared according to literature procedures.

Synthesis of 6-(4-octyloxyphenyl)-2,2'-bipyridine (1)

A mixture of *N*-(2-pyridacyl)pyridinium iodide (3.4 g, 10 mmol), 3-dimethylamino-1-(4-octyloxyphenyl)propan-1-one hydrochloride (3.3 g, 10 mmol), and NH_4OAc (17 g, 0.22 mol) in glacial acetic acid (40 mL) was refluxed under Ar for 3 days. After the addition of water and dichloromethane to the resulting mixture, the organic phase was washed with saturated $NaHCO_3$ aqueous solution, and brine, and then dried over Na_2SO_4. The solvent was evaporated in vacuo and the residue was chromatographed on silica-gel column (eluent, CH_2Cl_2/EtOAc 49:1) to give the desired 6-(4-octyloxyphenyl)-2,2'-bipyridine (**1**) (2.0 g, 5.5 mmol) as a white solid.

1: yield 55%; mp 61-62 °C; IR (KBr) 3279, 3048, 2917, 2850, 1607, 1582, 1561, 1516, 1455, 1434, 1249, 1182, 1017 cm^{-1}; ^{1}H NMR (400 MHz, $CDCl_3$, 1.0 x 10^{-2} M) δ 8.69 (d, 1H, J = 4.0 Hz), 8.63 (d, 1H, J = 8.0 Hz), 8.31 (d, 1H, J = 8.0 Hz), 8.10 (d,

1H, *J* = 8.8 Hz), 7.90-7.80 (m, 2H), 7.71 (d, 1H, *J* = 8.0 Hz), 7.32 (dd, 1H, *J* = 8.0, 4.0 Hz), 7.02 (d, 1H, *J* = 8.8 Hz), 4.04 (t, 2H, *J* = 6.4 Hz), 1.86-1.79 (m, 2H), 1.52-1.45 (m, 2H), 1.42-1.26 (m, 8H), 0.90 (t, 2H, *J* = 6.8 Hz); ^{13}C NMR (100 MHz, $CDCl^3$, 1.0 x 10^{-2} M) 160.1, 156.5, 156.2, 155.5, 149.0, 137.6, 136.9, 131.7, 128.2, 123.7, 121.3, 119.5, 118.6, 114.7, 68.1, 31.8, 29.4, 29.3, 26.1, 22.7, 14.1 ppm; HRMS (FAB) *m/z* Calcd. for $C_{24}H_{29}N_2O$ (M^+), 361.2274; Found, 361.2281; Anal. Calcd. for $C_{24}H_{28}N_2O$: C, 79.96; H, 7.83; N, 7.77. Found: C, 79.94; H, 7.82; N, 7.67.

Synthesis of the platinum(II) complex 2

A mixture of **1** (100 mg, 0.28 mmol) and K_2PtCl_4 (165 mg, 0.40 mol) in a mixed solvent of acetonitrile (8.0 mL) and water (8.0 mL) was refluxed under Ar for 42 h. After the reaction was completed, the acetonitrile was evaporated. The product was extracted with dichloromethane and the organic phase was washed with water, and brine, and then dried over Na_2SO_4. The solvent was evaporated in vacuo and the residue was washed with methanol to give the desired platinum(II) complex **2** (138 mg, 0.23 mmol) as an orange solid.

2: yield 84%; mp 153-154 °C (decomp.); IR (KBr) 3052, 2925, 2853, 1591, 1544, 1435, 1263, 1203, 1034 cm^{-1}; ^{1}H NMR (400 MHz, $CDCl_3$, 1.0 x 10^{-2} M) δ 8.99 (d, 1H, *J* = 5.6, 1.6 Hz), 8.05 (dt, 1H, *J* = 8.0, 1.6 Hz), 7.90 (d, 1H, *J* = 8.0 Hz), 7.75 (t, 1H, *J* = 8.0 Hz), 7.62 (dd, 1H, *J* = 8.0, 5.6 Hz), 7.47 (d, 1H, *J* = 8.0 Hz), 7.35 (d, 1H, *J* = 8.0 Hz), 7.28 (d, 1H, *J* = 8.8 Hz), 7.13 (d, 1H, *J* = 2.8 Hz), 6.61 (dd, 1H, *J* = 8.8, 2.8 Hz), 4.03 (t, 2H, *J* = 6.4 Hz), 1.82-1.75 (m, 2H), 1.52-1.44 (m, 2H), 1.41-1.26 (m, 8H), 0.90 (t, 3H, *J* = 6.8 Hz); ^{13}C NMR (100 MHz, $CDCl_3$, 1.0 x 10^{-2} M) 166.8, 161.6, 157.8, 154.7, 149.3, 145.4, 139.8, 139.1, 138.7, 127.8, 126.5, 122.8, 119.7, 118.4, 117.0, 111.1,

68.3, 32.3, 29.8, 29.7, 26.5, 23.1, 14.3 ppm; HRMS (FAB) *m/z* Calcd. for $C_{24}H_{27}ClN_2OPt$ (M^+), 589.1454; Found, 589.1456; Anal. Calcd. for $C_{24}H_{27}ClN_2OPt \cdot 0.5H_2O$: C, 48.12; H, 4.71; N, 4.68. Found: C, 48.29; H, 4.44; N, 4.58.

Synthesis of the bioorganometallic platinum(II) complex U6Pt

To a dichloromethane (3.0 mL) solution of 6-ethynyl-1-octyluracil (50 mg, 0.20 mmol), **2** (59 mg, 0.10 mmol), and CuI (1.5 mg, 7.9 μmol) was added triethylamine (1.2 mL, 8.6 mmol) under Ar at room temperature in the dark. The resulting mixture was stirred at room temperature for 23 h and the solvent was evaporated. The residue was washed with methanol, and the bioorganometallic platinum(II) complex **U6Pt** was isolated as a dark red solid (76 mg, 95 μmol) by recrystalization from dichloromethane and methanol.

U6Pt: yield 95%; mp 240-241 °C (decomp.); IR (KBr) 3427, 2925, 2853, 2089, 1696, 1651, 1561, 1456, 1435, 1262, 1202, 1041 cm^{-1}; ^1H NMR (400 MHz, CD_2Cl_2, 2.0 x 10^{-3} M) δ 8.97 (dd, 1H, *J* = 5.2, 1.6 Hz), 8.28 (br, 1H), 8.11 (td, 1H, *J* = 7.6, 1.6 Hz), 7.95 (d, 1H, *J* = 7.6 Hz), 7.84 (t, 1H, *J* = 8.0 Hz), 7.63-7.57 (m, 2H), 7.52 (d, 1H, *J* = 8.0 Hz), 7.37 (d, 1H, *J* = 8.4 Hz), 7.18 (d, 1H, *J* = 2.4 Hz), 6.62 (dd, 1H, *J* = 8.4, 2.4 Hz), 5.83 (s, 1H), 4.22 (t, 2H, *J* = 7.6 Hz), 4.00 (t, 2H, *J* = 6.4 Hz), 1.87-1.75 (m, 4H), 1.50-1.11 (m, 20H), 0.89 (t, 3H, *J* = 6.8 Hz), 0.77 (t, 3H, *J* = 6.8 Hz); ^{13}C NMR (100 MHz, CD_2Cl_2, 2.0 x 10^{-3} M) 165.7, 163.2, 162.1, 158.6, 154.7, 152.1, 151.5, 143.6, 142.7, 140.0, 139.9, 139.4, 128.2, 126.9, 124.2, 123.3, 118.7, 117.0, 110.5, 103.2, 97.2, 68.3, 46.7, 32.3, 29.8, 29.7, 29.3, 27.3, 26.5, 23.1, 23.0, 14.3 ppm; HRMS (FAB) *m/z* Calcd. for $C_{38}H_{47}N_4O_3Pt^{194}$ (M^+), 801.3275; Found, 801.3268; Anal. Calcd. for $C_{38}H_{46}N_4O_3Pt_1 \cdot 0.5H_2O$: C, 56.28; H, 5.84; N, 6.91. Found: C, 56.47; H, 5.53; N, 6.96.

Synthesis of the bioorganometallic platinum(II) complex U5Pt

To a dichloromethane (4.0 mL) solution of 5-ethynyl-1-octyluracil (75 mg, 0.30 mmol), **2** (89 mg, 0.15 mmol), and CuI (1.8 mg, 9.5 μmol) was added triethylamine (1.8 mL, 13 mmol) under Ar at room temperature in the dark. The resulting mixture was stirred at room temperature for 14 h and the solvent was evaporated. The product was extracted with dichloromethane. After evaporation of the solution, the bioorganometallic platinum(II) complex **U5Pt** was isolated as an orange solid (73 mg, 91 μmol) by reprecipitation from dichloromethane and ether.

U5Pt: yield 61%; mp 197-199 °C (decomp.); IR (KBr) 3088, 3039, 2928, 2852, 2106, 1695, 1659, 1581, 1547, 1435, 1351, 1225, 1173 cm^{-1}; ^{1}H NMR (400 MHz, CD_2Cl_2, 2.5 x 10^{-3} M) δ 9.36 (d, 1H, *J* = 5.2 Hz), 8.32 (s, 1H), 8.07 (t, 1H, *J* = 7.6 Hz), 7.94 (d, 1H, *J* = 7.6 Hz), 7.80 (t, 1H, *J* = 8.0 Hz), 7.63 (dd, 1H, *J* = 7.6, 5.2 Hz), 7.58 (d, 1H, *J* = 8.0 Hz), 7.48 (d, 1H, *J* = 8.0 Hz), 7.44 (s, 1H), 7.39 (d, 1H, *J* = 2.4 Hz), 7.37 (d, 1H, *J* = 8.4 Hz), 6.60 (dd, 1H, *J* = 8.4, 2.4 Hz), 4.07 (t, 2H, *J* = 6.4 Hz), 3.72 (t, 2H, *J* = 7.2 Hz), 1.83-1.68 (m, 4H), 1.52-1.25 (m, 20H), 0.91-0.87 (m, 6H); ^{13}C NMR (100 MHz, CD_2Cl_2, 2.5 x 10^{-3} M) 165.7, 163.4, 162.1, 158.7, 154.9, 152.5, 150.2, 144.8, 143.7, 139.6, 139.4, 139.3, 128.2, 126.6, 124.0, 122.9, 118.4, 116.9, 112.6, 110.3, 104.8, 94.7, 68.3, 49.1, 32.3, 32.2, 29.9, 29.8, 29.7, 29.6, 29.5, 26.9, 26.5, 23.1, 23.0, 14.3, 14.2 ppm; HRMS (FAB) *m/z* Calcd. for $C_{38}H_{47}N_4O_3Pt^{194}$ (M^+), 801.3275; Found, 801.3267; Anal. Calcd. for $C_{38}H_{46}N_4O_3Pt_1 \bullet 0.5H_2O$: C, 56.28; H, 5.84; N, 6.91. Found: C, 56.49; H, 5.55; N, 6.98.

Synthesis of 2,6-dihexamido-4-ethynylpyridine (7)

2,6-Dihexamido-4-ethynylpyridine (**7**) was synthesized from 4-benzyloxy-2,6-pyridinediamine in 5 steps. To a dichloromethane (100 mL) solution of 4-benzyloxy-2,6-pyridinediamine (2.2 g, 10 mmol) and triethylamine (5.6 mL, 40 mmol) was added a dichloromethane (50 mL) solution of heptanoylchloride (3.3 mL, 21 mmol) dropwise under Ar at 0 °C. The resulting mixture was stirred at room temperature for 12 h. The resulting mixture was diluted with dichloromethane, washed with saturated $NaHCO_3$ aqueous solution and brine, and then dried over Na_2SO_4. The solvent was evaporated in vacuo and the residue was chromatographed on silica-gel column (eluent, CH_2Cl_2) to give **3** (3.3 g, 7.6 mmol).

3: yield 76%; mp 54-56 °C; IR (KBr) 3424, 3325, 2953, 2926, 2860, 2367, 1692, 1673, 1583, 1541, 1503, 1440 cm^{-1}; ^1H NMR (400 MHz, CD_2Cl_2, 5.0 x 10^{-2} M) δ 7.66 (s, 2H), 7.61 (s, 2H), 7.46-7.32 (m, 5H), 5.14 (s, 2H), 2.33 (t, J = 7.5 Hz, 4H), 1.70-1.63 (m, 4H), 1.38-1.28 (m, 12H), 0.89 (t, J = 7.0 Hz, 6H); ^{13}C NMR (100 MHz, CD_2Cl_2, 5.0 x 10^{-2} M) 172.0, 168.8, 151.3, 136.5, 128.9, 128.5, 128.1, 96.2, 70.5, 38.1, 31.9, 29.2, 25.6, 22.9, 14.2 ppm; HRMS (FAB) *m/z* Calcd. for $C_{26}H_{38}N_3O_3$ (M^+), 440.2908; Found, 440.2924.

Benzyl ether **3** (5.6 g, 13 mmol) was dissolved in a mixture of ethanol (60 mL). Pd/C (10 weight%, 0.59 g) was added and the reaction mixture was placed under H_2, stirred at room temperature for 18 h and filtered through celite. The solvent was evaporated in vacuo and the residue was chromatographed on silica-gel column (eluent, EtOAc) to give **4** (4.0 g, 12 mmol).

4: yield 90%; mp 80-82 °C; IR (KBr) 3271, 2956, 2929, 2858, 1657, 1597, 1464, 1435, 1230 cm^{-1}; ^1H NMR (400 MHz, $CDCl^3$, 1.0 x 10^{-2} M) δ 10.03 (s, 1H), 7.67

(s, 2H), 7.55 (s, 2H), 2.38 (t, J = 7.6 Hz, 4H), 1.75-1.68 (m, 4H), 1.41-1.25 (m, 12H), 0.89 (t, J = 6.4 Hz, 6H); ^{13}C NMR (100 MHz, $CDCl_3$, 1.0 x 10^{-2} M) 172.6, 168.0, 150.1, 98.0, 38.1, 31.5, 28.8, 25.4, 22.5, 14.0 ppm; HRMS (FAB) *m/z* Calcd. for $C_{19}H_{32}N_3O_3$ (M^+), 350.2438; Found,350.2454; Anal. Calcd. for $C_{19}H_{31}N_3O_3$: C, 65.30; H, 8.94; N, 12.02. Found: C, 65.05; H, 8.94; N, 11.84.

To a pyridine (6.5 mL, 80 mmol) solution of **4** (700 mg, 2.0 mmol) was added trifluoromethanesulfonic anhydride (0.5 mL, 3.0 mmol) dropwise under Ar at 0 °C. The reaction mixture was stirred at room temperature for 3 h. After removal of the solvent, the residue was poured into water and extracted with diethyl ether. The diethyl ether extract was evaporated in vacuo and the residue was chromatographed on silica-gel column (eluent, hexane/EtOAc 4:1) to give **5** (810 mg, 1.7 mmol).

5: yield 84%; mp 49-51 °C; IR (KBr) 3396, 3261, 3120, 3040, 2958, 2931, 2862, 2362, 1686, 1605, 1523, 1433, 1212 cm^{-1}; ^{1}H NMR (400 MHz, CD_2Cl_2, 5.0 x 10^{-2} M) δ 7.93 (s, 2H), 7.80 (s, 2H), 2.38 (t, J = 7.7 Hz, 4H), 1.73-1.64 (m, 4H), 1.40-1.29 (m, 12H), 0.89 (t, J = 7.0 Hz, 6H); ^{13}C NMR (100 MHz, CD_2Cl_2, 5.0 x 10^{-2} M) 172.2, 159.0, 151.8, 119.0, 101.9, 38.0, 31.9, 29.2, 25.4, 22.9, 14.2 ppm; HRMS (FAB) *m/z* Calcd. for $C_{20}H_{31}F_3N_3O_5S_1$ (M^+), 482.1931; Found, 482.1949

To a triethylamine (24 mL) solution of **5** (1.9 g, 4.0 mmol), $PdCl_2(Ph_3P)_2$ (0.14 g, 0.20 mmol), and CuI (19 mg, 0.10 mmol) was added (trimethylsilyl)acetylene (2.8 mL, 20 mmol) under Ar at room temperature. The reaction mixture was stirred at 50 °C for 14 h. After removal of the solvent, the residue was poured into water and extracted with dichloromethane. The dichloromethane extract was evaporated in vacuo and the residue was chromatographed on silica-gel column (eluent, CH_2Cl_2) to give **6** (1.7 g, 3.9 mmol).

6: yield 98%; IR (KBr) 3282, 2958, 2947, 2858, 2168, 1675, 1609, 1557, 1419, 1211 cm^{-1}; ^{1}H NMR (400 MHz, CD_2Cl_2, 5.0 x 10^{-2} M) δ 7.93 (s, 2H), 7.86 (s, 2H), 2.34 (t, *J* = 7.6 Hz, 4H), 1.70-1.62 (m, 4H), 1.36-1.27 (m, 12H), 0.88 (t, *J* = 7.0 Hz, 6H), 0.24 (s, 9H); ^{13}C NMR (100 MHz, CD_2Cl_2, 5.0 x 10^{-2} M) 172.0, 150.3, 135.6, 111.6, 102.8, 99.7, 38.0, 31.9, 29.2, 25.6, 22.9, 14.2, -0.3 ppm; HRMS (FAB) *m/z* Calcd. for $C_{24}H_{40}N_3O_2Si_1$ (M^+), 430.2884; Found, 430.2899.

A mixture of **6** (1.6 g, 3.7 mmol) and KOH (0.41 g, 7.3 mmol) in methanol (55 mL) was stirred at room temperature under Ar for 4 h. The resulting mixture was diluted with ethyl acetate, washed with water and brine, and then dried over Na_2SO_4. The ethyl acetate extract was evaporated in vacuo and the residue was chromatographed on silica-gel column (eluent, CH_2Cl_2/EtOAc 9:1) to give **7** (0.98 g, 2.7 mmol).

7: yield 73%; mp 45-47 °C; IR (KBr) 3566, 3402, 3278, 2955, 2927, 2857, 2116, 1672, 1613, 1557, 1507, 1419, 1212 cm^{-1}; ^{1}H NMR (400 MHz, CD_2Cl_2, 5.0 x 10^{-2} M) δ 7.97 (s, 2H), 7.67 (s, 2H), 3.31 (s, 1H), 2.35 (t, *J* = 7.6 Hz, 4H), 1.72-1.64 (m, 4H), 1.38-1.29 (m, 12H), 0.89 (t, *J* = 7.0 Hz, 6H); ^{13}C NMR (100 MHz, CD_2Cl_2, 5.0 x 10^{-2} M) 171.9, 150.4, 134.7, 111.9, 81.8, 81.5, 38.1, 31.9, 29.2, 25.6, 22.9, 14.2 ppm; HRMS (FAB) *m/z* Calcd. for $C_{21}H_{32}N_3O_2$ (M^+), 358.2489; Found, 358.2499; Anal. Calcd. for $C_{21}H_{31}N_3O_2 \bullet 0.5H_2O$: C, 68.82; H, 8.80; N, 11.47. Found: C, 68.78; H, 8.76; N, 11.19.

Synthesis of the molecular scaffold ND

To a DMF (7.5 mL) solution of 1,8-diiodonaphthalene (92 mg, 0.24 mmol), **7** (0.26 g, 0.72 mmol), $PdCl_2(Ph_3P)_2$ (15 mg, 20 μmol), and CuI (4.8 mg, 25 μmol) was added triethylamine (2.5 mL, 18 mmol) at room temperature. The resulting mixture was stirred under Ar at 55 °C for 21 h. The resulting mixture was diluted with dichloromethane, washed with water and brine, and then dried over Na_2SO_4. The solvent was evaporated in vacuo and the residue was chromatographed on silica-gel column (eluent, $CHCl_3$/EtOAc 19:1) to give **ND** (79 mg, 95 μmol) as a white solid.

ND: yield 40%; mp 178-180 °C; IR (KBr) 3296, 3050, 2954, 2928, 2856, 2211, 1703, 1672, 1610, 1555, 1420, 1260, 1213, 1168 cm^{-1}; ^1H NMR (400 MHz, $CDCl_3$, 5.0 x 10^{-3} M) δ 7.95-7.91 (m, 4H), 7.77 (s, 4H), 7.55-7.52 (m, 6H), 2.30 (t, 8H, J = 7.7 Hz, H), 1.65(q, J = 7.7 Hz, 8H), 1.39-1.28 (m, 24H), 0.90 (t, J = 7.0 Hz, 12H); ^{13}C NMR (100 MHz, $CDCl_3$, 5.0 x 10^{-3} M) 171.3, 149.8, 136.1, 135.9, 134.4, 131.7, 130.9, 126.2, 120.0, 111.5, 95.1, 93.9, 37.9, 32.0, 29.3, 25.6, 22.9, 14.2 ppm; HRMS (FAB) *m/z* Calcd. for $C_{53}H_{67}N_6O_4$ (M^+), 839.5218; Found, 839.5220; Anal. Calcd. for $C_{52}H_{66}N_6O_4 \cdot H_2O$: C, 72.87; H, 8.00; N, 9.80. Found: C, 73.14; H, 7.78; N, 9.69.

Synthesis of the molecular scaffold AD

To a tetrahydrofuran (3.5 mL) solution of 1,8-diethynylanthracene (91 mg, 0.40 mmol), **5** (0.48 g, 1.0 mmol), $PdCl_2(Ph_3P)_2$ (8.4 mg, 12 μmol), and CuI (2.3 mg, 12 mol) was added triethylamine (1.5 mL, 11 mmol) at room temperature. The resulting mixture was stirred under Ar at 50 °C for 17 h. The resulting mixture was diluted with dichloromethane, washed with water and brine, and then dried over Na_2SO_4. The solvent was evaporated in vacuo and the residue was chromatographed on silica-gel

column (eluent, CH_2Cl_2/MeOH 19:1) to give **AD** (98 mg, 0.11 mmol) as a pale yellow solid.

AD: yield 28%; mp 213-215 °C; IR (KBr) 3057, 2955, 2927, 2856, 2208, 1708, 1609, 1556, 1501, 1418, 1264, 1212, 1166 cm^{-1}; ^1H NMR (400 MHz, CD_2Cl_2, 5.0 x 10^{-3} M) δ 9.56 (s, 1H), 8.56 (s, 1H), 8.12 (d, *J* = 8.8 Hz, 2H), 7.98 (s, 4H), 7.88 (d, *J* = 6.8 Hz, 2H), 7.55 (dd, *J* = 8.8, 6.8 Hz, 2H), 2.27 (t, *J* = 7.6 Hz, 8H), 1.65-1.56 (m, 8H), 1.37-1.26 (m, 24H), 0.91 (t, *J* = 6.8 Hz, 12H); ^{13}C NMR (100 MHz, CD_2Cl_2, 5.0 x 10^{-3} M) 171.4, 150.1, 135.8, 132.0, 131.9, 131.8, 130.3, 128.2, 125.7, 124.3, 120.9, 111.6, 93.7, 91.9, 37.9, 32.0, 29.4, 25.5, 23.0, 14.2 ppm; HRMS (FAB) *m/z* Calcd. for $C_{56}H_{69}N_6O_4$ (M^+), 889.5375; Found, 889.5370.

Physical measurements

UV/vis spectra were obtained using a Hitachi U-3500 spectrophotometer in a deaerated dichloromethane solution under nitrogen at 298 K. Emission spectra were collected using a Shimadzu RF-5300PC spectrofluorophotometer in a deaerated dichloromethane solution under nitrogen at 298 K.

^{1}H NMR titrations

The CD_2Cl_2 solution of **ND** or **AD** with a concentration 0.5 x 10^{-3} M containing various amounts of **U6Pt** or **U5Pt** was prepared and ^1H NMR spectra were measured at 295 K. The changes in chemical shift of **ND** or **AD** signals as a function of **U6Pt** or **U5Pt** were then analyzed. Titration data for three different signals were used to determine the association constant in each experiment.

Job's plots

For each component of the complex, 5.0 mL CD_2Cl_2 solutions of accurately measured and identical concentrations (2.0 x 10^{-3} M) were prepared. The two solutions were then combined to give a series of samples of identical total concentration (2.0 x 10^{-3} M) containing different mole fractions of the two components. The ^{1}H NMR spectrum of each sample was then measured at 295 K, and these spectra were used to produce a graph of $\Delta\delta$ x [H] against [H]/([H] + [G]) shown as the Job's plots.

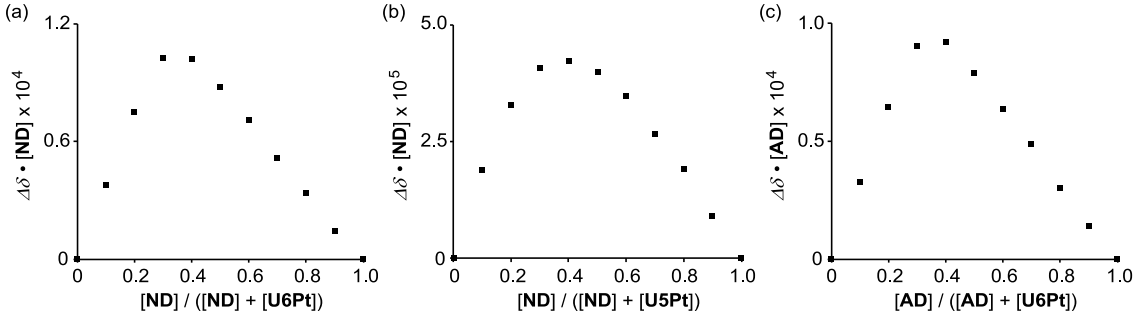

Figure 8. (a) Job's plots for complexation of **ND** with **U6Pt**, where $\Delta\delta$ x [**ND**] was plotted against [**ND**]/([**ND**] + [**U6Pt**]) at an invariant total concentration of 2.0 x 10^{-3} M in CD_2Cl_2 at 295 K, (b) Job's plots for complexation of **AD** with **U6Pt**, where $\Delta\delta$ x [**AD**] was plotted against [**AD**]/([**AD**] + [**U6Pt**]) at an invariant total concentration of 2.0 x 10^{-3} M in CD_2Cl_2 at 295 K and (c) Job's plots for complexation of **ND** with **U5Pt**, where $\Delta\delta$ x [**ND**] was plotted against [**ND**]/([**ND**] + [**U5Pt**]) at an invariant total concentration of 2.0 x 10^{-3} M in CD_2Cl_2 at 295 K.

X-ray structure analysis

All measurements for **U6Pt** were made on a Rigaku R-AXIS RAPID diffractometer using graphite monochromated Mo Kα radiation. The structure of **U6Pt** was solved by direct methods[9] and expanded using Fourier techniques. All calculations were performed using the CrystalStructure crystallographic software package[10] except for the refinement, which was performed using SHELXL-97.[11] The non-hydrogen atoms were refined anisotropically. The H atoms involved in hydrogen bonding were located in electron density maps. The remainder of the H atoms were placed in idealized positions and allowed to ride with the C atoms to which each was bonded. Crystallographic details are given in Table 2. Selected bond distances and angles of **U6Pt** are reported in Table 3. Crystallographic data (excluding structure factors) for the structures reported in this paper have been deposited with the Cambridge Crystallographic Data Centre as supplementary publication no. CCDC-851423 for **U6Pt**. Copies of the data can be obtained free of charge on application to CCDC, 12 Union Road, Cambridge CB2 1EZ, UK [Fax: (internat.) +44-1223/336-033; E-mail: deposit@ccdc.cam.ac.uk].

Table 2. Crystallographic data for **U6Pt**

	U6Pt
Formula	$C_{38.5}H_{47}N_4O_3Pt_1Cl_1$
Molecular weight	844.36
Crystal system	Triclinic
Space group	*P*-1 (No. 2)
a (Å)	12.1080(4)
b (Å)	14.5494(5)
c (Å)	20.4353(7)
α (°)	89.7533(9)
β (°)	88.4541(9)
γ (°)	83.7668(9)
V (Å^3)	3577.4(2)
Z	4
D_{calcd} (g cm^{-3})	1.568
μ (Mo Ka) (cm^{-1})	40.236
T (°C)	–150
λ (Mo Kα) (Å)	0.71075
*R*1[a]	0.065
*wR*2[b]	0.214

(a) $R1 = \Sigma||F_o| - |F_c|| / \Sigma|F_o|$.

(b) $wR2 = [\Sigma w(F_o^2 - F_c^2)^2 / \Sigma w(F_o^2)^2]^{1/2}$.

Table 3. Selected bond distances (Å) and angles (°) for **U6Pt**

	U6Pt	
Bond distances (Å)		
Pt(1)–N(1)	2.112(9)	2.141(9)
Pt(1)–N(2)	1.983(8)	1.985(8)
Pt(1)–C(16)	2.010(11)	2.010(9)
Pt(1)–C(25)	1.949(9)	1.931(9)
O(2)–C(28)	1.234(12)	1.225(12)
O(3)–C(29)	1.234(12)	1.259(12)
N(3)–C(27)	1.390(13)	1.394(13)
N(3)–C(28)	1.399(12)	1.397(12)
N(4)–C(28)	1.358(13)	1.373(13)
N(4)–C(29)	1.389(12)	1.371(13)
C(25)–C(26)	1.211(13)	1.220(13)
C(26)–C(27)	1.437(13)	1.419(13)
C(27)–C(30)	1.340(14)	1.344(14)
C(29)–C(30)	1.433(12)	1.409(13)
Bond angles (°)		
N(1)–Pt(1)–N(2)	77.8(4)	79.1(4)
N(1)–Pt(1)–C(16)	160.3(4)	160.7(4)
N(1)–Pt(1)–C(25)	101.2(4)	99.8(4)
N(2)–Pt(1)–C(16)	82.5(4)	81.7(4)
N(2)–Pt(1)–C(25)	176.3(4)	178.8(4)
C(16)–Pt(1)–C(25)	98.4(4)	99.5(4)
N(3)–C(28)–N(4)	116.3(9)	114,7(8)
N(4)–C(29)–C(30)	114.7(8)	114.8(9)
C(27)–N(3)–C(28)	121.0(8)	122.1(8)
C(27)–N(3)–C(29)	125.9(8)	126.7(8)

(a) Two independent molecules exist in an asymmetric unit.

1-5. References

1. (a) D. M. Roundhill, H. B. Gray and C.-M. Che, *Acc. Chem. Res.*, 1989, **22**, 55; (b) V. H. Houlding and V. M. Miskowski, *Coord. Chem. Rev.*, 1991, **111**, 145; (c) M. Kato, *Bull. Chem. Soc. Jpn.*, 2007, **80**, 287; (d) I. Eryazici, C. N. Moorefield and G. R. Newkome, *Chem. Rev.*, 2008, **108**, 1834; (e) J. A. G. Williams, S. Develay, D. L. Rochester and L. Murphy, *Coord. Chem. Rev.*, 2008, **252**, 2596; (f) R. McGuire Jr., M. C. McGuire and D. R. McMillin, *Coord. Chem. Rev.*, 2010, **254**, 2574; (g) K. M.-C. Wong and V. W.-W. Yam, *Acc. Chem. Res.*, 2011, **44**, 424.
2. (a) G. A. Jeffrey, *An introduction to hydrogen bonding*, 1st ed. Oxford University Press, New York, 1997; (b) M. M. Conn and J. Rebek, Jr., *Chem. Rev.*, 1997, **97**, 1647; (b) E. A. Archer, H. Gong and M. J. Krische, *Tetrahedron*, 2001, **57**, 1139; (c) L. J. Prins, D. N. Reinhoudt and P. Timmerman, *Angew. Chem. Int. Ed.*, 2001, **40**, 2382.
3. Self-association constants (K_{dim}) of **U6Pt** and **U5Pt** were calculated to be less than 20 M^{-1}, suggesting that self-association would not interfere with aggregation of the organoplatinum(II) compounds to the molecular scaffolds.
4. T. Moriuchi, S. Noguchi, Y. Sakamoto and T. Hirao, *J. Organomet. Chem.*, 2011, **696**, 1089.
5. M. Takase and M. Inouye, *J. Org. Chem.*, 2003, **68**, 1134.
6. T. Braxmeier, M. Demarcus, T. Fessmann, S. McAteer and J. D. Kilburn, *Chem. Eur. J.*, 2001, **7**, 1889.
7. H. O. House, D. G. Koepsell and W. J. Campbell, *J. Org. Chem.*, 1972, **37**, 1003.
8. H. E. Katz, *J. Org. Chem.*, 1989, **54**, 2179.
9. A. Altomare, M. C. Burla, M. Camalli, G. L. Cascarano, C. Giacovazzo, A. Guagliardi, A. G. G. Moliterni, G. Polidori and R. Spagna, *J. Appl. Cryst.*, 1999, **32**, 115.
10. CrystalStructure 4.0: Crystal Structure Analysis Package, Rigaku Corporation (2000-2010). Tokyo 196-8666, Japan.
11. G. M. Sheldrick, *Acta Crystallogr., Sec. A* 2008, **64**, 112.

Chapter 2. Synthesis and structural properties of mononuclear organogold(I) complexes bearing uracil moieties

2-1. Introduction

Organogold(I) complex has drawn increasing attention because of their aggregation properties through an attractive aurophilic interaction.[1] This aurophilic interaction possesses the comparable strength to a hydrogen bonding and is useful for construction of supramolecular architectures in a solid state. A combination of organogold(I) complexes with nucleobases is envisaged to provide highly-organized assembly bioorganometallic systems depending on both properties. Herein I report the structural characterization of organogold(I)-uracil conjugates to disclose the steric effects of ancillary ligands on assembly properties of the uracil and the gold(I) moieties in a solid state.

2-2. Results and discussion

The organogold(I)-uracil conjugates were designed by introduction of planar phenyl isocyanide and bulky triphenylphosphine as an ancillary ligand to clarify the effect of ancillary ligands on the assembly properties. The synthesis of organogold(I)-uracil conjugates **U6AuCNPh** and **U6AuPPh$_3$** is depicted in Scheme 1. The organogold(I)-uracil conjugate bearing planar phenyl isocyanide **U6AuCNPh** was obtained by the coupling reaction of 6-ethynyl-1-octyluracil with chloro(phenyl isocyanide)gold(I) [(PhNC)AuCl], which was prepared by the treatment of chloro(tetrahydrothiophene)gold(I) [(tht)AuCl] with phenyl isocyanide, in the presence of CuI as a catalyst. The reaction of 6-ethynyl-1-octyluracil with

chloro(triphenylphosphine)gold(I), which was prepared by the treatment of chloro(tetrahydrothiophene)gold(I) with triphenylphosphine *in situ*, in the presence of sodium bis(trimethylsilyl)amide produced the organogold(I)-uracil conjugate bearing bulky triphenylphosphine **U6AuPPh$_3$**. The formation of thus-obtained organogold(I)-uracil conjugates was confirmed by ^{1}H NMR, ^{13}C NMR, ^{31}P NMR, IR, HRMS, and elemental analysis. For example, the uracil proton showed upfield shift in the ^{1}H NMR spectra after the introduction of the gold(I) center.

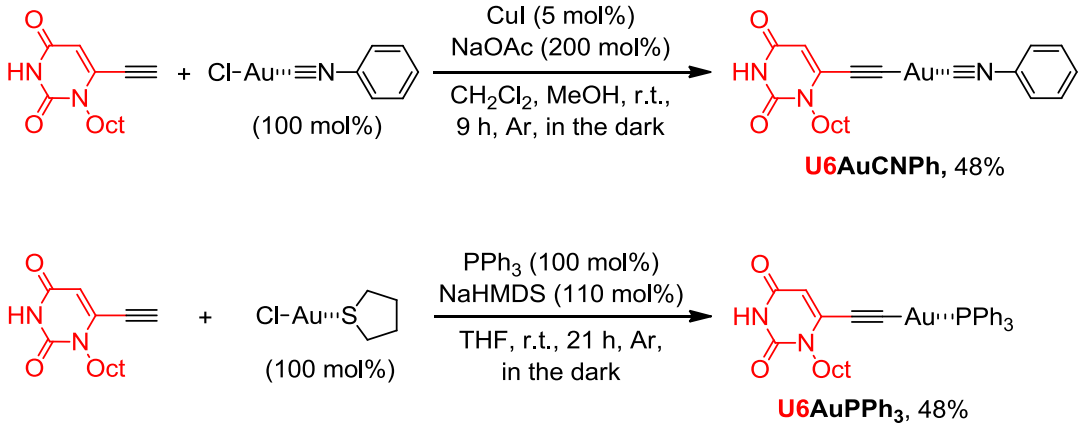

Scheme 1.

The structural features of **U6AuCNPh** and **U6AuPPh$_3$** were confirmed by single-crystal X-ray structure determination, revealing the self-assembly properties of the gold(I) and uracil moieties. The crystal structure of **U6AuCNPh** possess propeller twist conformation with a dihedral angle of 45.9(4)° between the planes of the uracil and benzene moieties of phenyl isocyanide (Figure 1a). It is noteworthy that a head-to-tail dimer through the Au(I)-Au(I) and π–π interactions between the uracil and benzene moieties of phenyl isocyanide was formed in a crystal packing as shown in

Figure 1b. Furthermore, each head-to-tail dimer was linked with not only the intermolecular hydrogen bonds of N-H•••O pattern between the uracil moieties but the weak hydrogen bonds of C-H•••O pattern between the uracil and benzene moieties of phenyl isocyanide (Figure 1c and Table 1).

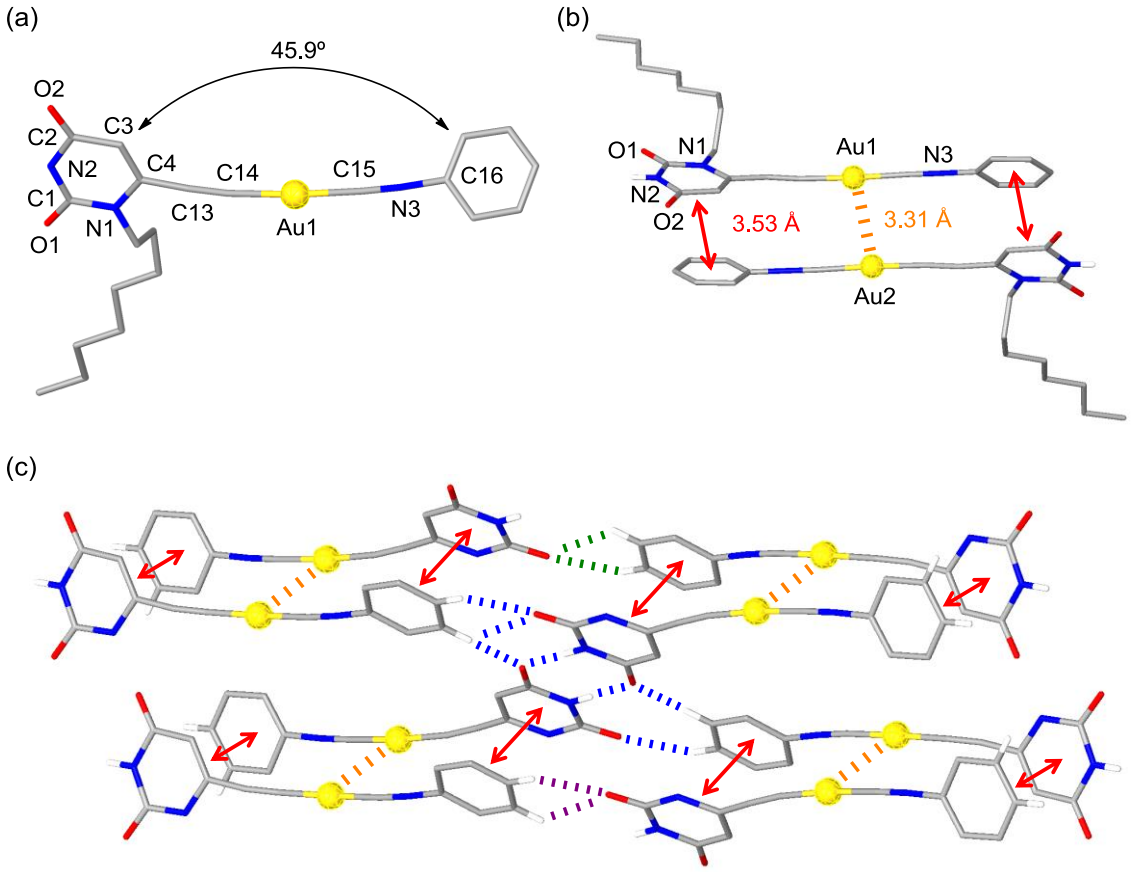

Figure 1. (a) Molecular structure, (b) a head-to-tail dimer, and (c) a part of the intermolecular hydrogen bonds of N-H•••O pattern between the uracil moieties and the weak hydrogen bonds of C-H•••O pattern between the uracil and benzene moieties of phenyl isocyanide of **U6AuCNPh** (octyl moieties are omitted for clarity).

Table 1. Intermolecular hydrogen bonds for **U6AuCNPh** and **U6AuPPh$_3$**[a]

Compounds	Donor	Acceptor	D•••A (Å)	D–H•••A (°)
U6AuCNPh	N(2)	O(2)[b]	2.827(12)	160(11)
	C(19)	O(1)[c]	3.159(14)	125.2(8)
	C(20)	O(1)[c]	3.210(13)	119.0(8)
	C(20)	O(2)[d]	3.468(15)	146.2(2)
U6AuPPh$_3$	N(2)	O(52)[e]	2.854(9)	168(5)
	N(52)	O(2)[e]	2.849(8)	168(3)

(a) Two independent molecules exist in an asymmetric unit. (b) –X, –Y, –Z–1.

(c) X, Y+1/2, –Z. (d) –X, –Y+1/2, Z+1. (e) –X+1/2, –Y+1/2, –Z+1.

The organogold(I)-uracil conjugate **U6AuPPh$_3$** crystallized in the space group *C*2/*c* (*Z* = 16) and two independent molecules of **U6AuPPh$_3$** exist in an asymmetric unit. The structural characterization of **U6AuPPh$_3$** is confirmed by the formation of the dimeric structure through intermolecular hydrogen bonds of N-H•••O pattern between the uracil moieties of two independent molecules as shown in Figure 2. Self-assembly properties of the organogold(I)-uracil conjugates were found to depend on the ancillary ligands. In comparison with the self-assembly properties of **U6AuCNPh**, the crystal structure of **U6AuPPh$_3$** showed no Au(I)-Au(I) interaction probably due to the sterically bulky triphenylphosphine ligand (Figure 2b).

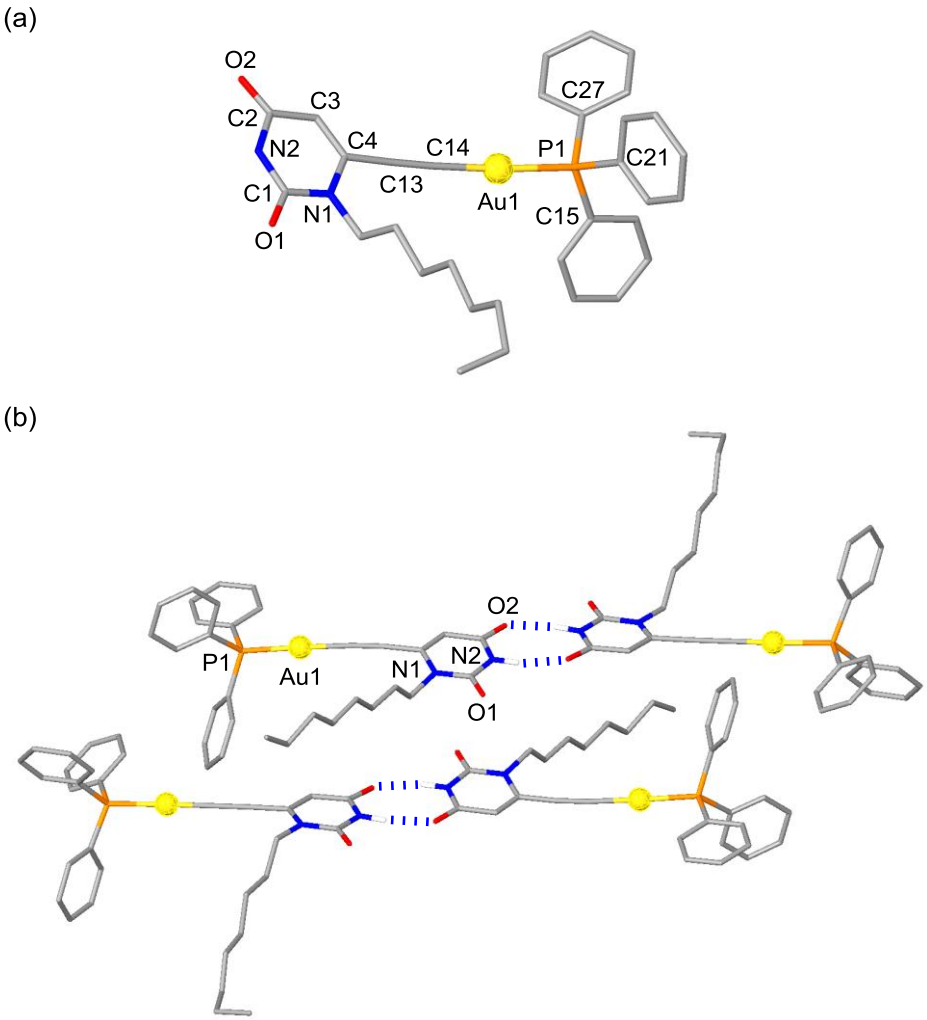

Figure 2. (a) Molecular structure and (b) a hydrogen-bonded dimer through intermolecular hydrogen bonds between the uracil moieties of **U6AuPPh$_3$**.

2-3. Conclusions

The bioorganometallic compounds consisted of the organogold(I) complexes with uracil moiety as a nucleobase were designed and synthesized. The structural characterization of organogold(I)-uracil conjugates was demonstrated to disclose the assembly properties of the gold(I) and the uracil moieties in a solid state. Interesting feature of organogold(I)-uracil conjugates is their strong tendency to self-assemble through intermolecular hydrogen bonds, wherein hydrogen bonding patterns were found to depend on the ancillary ligands. Furthermore, the introduction of planar phenyl isocyanide as an ancillary ligand induced the formation of a head-to-tail dimer through the Au(I)-Au(I) and π–π interactions between the uracil and the benzene moieties of phenyl isocyanide. On the contrary, the Au(I)-Au(I) interaction was not observed in the case of bulky triphenylphosphine ancillary ligand probably due to the steric hindrance.

2-4. Experimental section

General methods

All reagents and solvents were purchased from commercial sources and were further purified by the standard methods, if necessary. 6-ethynyl-1-octyluracil,[2] chloro(tetrahydrothiophene)gold(I) [(tht)AuCl][3] and chloro(phenyl isocyanide)gold(I) [(PhNC)AuCl][4] were prepared by the literature methods. Infrared spectra were obtained with a JASCO FT/IR-6200 spectrometer. ^{1}H, ^{13}C, and ^{31}P NMR spectra were recorded on a JNM-ECS 400 (400, 100, and 160 MHz, respectively) spectrometer. For ^{1}H and ^{31}P NMR spectra, chemical shifts were determined by using of tetramethylsilane and 85% H_3PO_4 aq. as standard samples, respectively. Chemical shifts of ^{13}C NMR spectra were determined relative to the solvent residual peaks. Mass spectra were run on a JEOL JMS-700 mass spectrometer.

Synthesis of (1-octyluracil-6-)ethynyl(phenyl isocyanide)gold(I) U6AuCNPh

To a mixture of chloro(phenyl isocyanide)gold(I) (67 mg, 0.20 mmol), 6-ethynyl-1-octyluracil (50 mg, 0.20 mmol), CuI (1.9 mg, 10 μmol), and NaOAc (33 mg, 0.40 mmol) were added dichloromethane (16 mL) and methanol (4.0 mL). The resulting mixture was stirred at room temperature for 9 h under Ar in the dark. The solvent was evaporated and the residue was extracted with dichloromethane, insoluble impurities was filtered out. The solvent was evaporated and purification of the crude product by recrystallization from dichloromethane, diethyl ether, and hexane gave the desired gold(I) complex **U6AuCNPh** (53 mg, 0.096 mmol) as a pale yellow crystal.

U6AuCNPh: yield 48%; IR (KBr) 3150, 2924, 2855, 2228, 2124, 1712, 1656, 1574, 1465, 1416, 1364 cm^{-1}; ^{1}H NMR (400 MHz, CD_2Cl_2, 4.0 x 10^{-2} M): δ 8.97 (br,

1H), 7.64-7.52 (m, 5H), 5.73 (s, 1H), 4.03 (t, 1H, J = 7.6 Hz), 1.38-1.29 (m, 10H), 1.50-1.11 (m, 20H), 0.89 (t, 3H, J = 6.8 Hz); ^{13}C NMR (100 MHz, CD_2Cl_2, 4.0 x 10^{-2} M): 163.4, 155.0 (t, J = 24.9 Hz), 151.4, 140.2, 140.0, 132.3, 130.5, 127.4, 124.6 (t, J = 14.4 Hz), 105.7, 93.7, 46.7, 32.4, 29.7, 29.6, 28.9, 27, 23.2, 14.4 ppm; HRMS (FAB) *m/z* Calcd. for $C_{21}H_{25}N_3O_2Au$ (M + H^+), 548.1607; found, 548.1612; Anal. Calcd. for $C_{21}H_{24}N_3O_2Au$: C, 46.08; H, 4.42; N, 7.68. Found: C, 45.78; H, 4.37; N, 7.68.

Synthesis of (1-octyluracil-6-)ethynyl(triphenylphosphine)gold(I) U6AuPPh$_3$

A mixture of triphenylphosphine (53 mg, 0.20 mmol), chloro(tetrahydrothiophene)gold(I) (64 mg, 0.20 mmol), and 6-ethynyl-1-octyluracil (50 mg, 0.20 mmol) was stirred in THF (10 mL) at room temperature for 15 minutes under Ar. To the solution was added sodium bis(trimethylsilyl)amide (40 mg, 0.22 mmol) and the resulting solution was stirred at room temperature under Ar for 21 h. The mixture was diluted with dichloromethane, washed with water, brine, and then dried over Na_2SO_4. The solvent was evaporated and purification of the crude product by recrystallization from dichloromethane, diethyl ether, and hexane gave the desired gold(I) complex **U6AuPPh$_3$** (68 mg, 0.096 mmol) as a colorless crystal.

U6AuPPh$_3$: yield 48%; IR (KBr) 3170, 3074, 2923, 2852, 2116, 1698, 1661, 1574, 1456, 1402, 1366 cm^{-1}; ^{1}H NMR (400 MHz, CD_2Cl_2, 1.0 x 10^{-2} M): δ 8.30 (br, 1H), 7.59-7.48 (m, 15H), 5.74 (s, 1H), 4.06 (t, 2H, J = 7.6 Hz), 1.77-1.69 (m, 2H), 1.41-1.21 (m, 10H), 0.80 (t, 3H, J = 6.8 Hz); ^{13}C NMR (100 MHz, CD_2Cl_2, 1.0 x 10^{-2} M): 163, 151.4 (d, $^2J_{C\text{-}P}$ = 142.3 Hz), 151.2, 140.3 (d, $^4J_{C\text{-}P}$ = 3.1 Hz), 134.6 (d, $^2J_{C\text{-}P}$ = 13.7 Hz), 132.2 (d, $^4J_{C\text{-}P}$ = 2.2 Hz), 129.6 (d, $^3J_{C\text{-}P}$ = 11.3 Hz), 129.6 (d, $^1J_{C\text{-}P}$ = 57 Hz), 105.2, 93.8 (d, $^3J_{C\text{-}P}$ = 26.6 Hz), 46.7, 32.2, 29.6, 29.5, 28.9, 27, 23, 14.2 ppm; ^{31}P NMR

(160 MHz, CD_2Cl_2, 1.0 x 10^{-2} M): 41.8 ppm; HRMS (FAB) *m/z* Calcd for $C_{32}H_{35}N_2O_2PAu$ ($M + H^+$), 707.2096; Found, 707.2096; Anal. Calcd. for $C_{32}H_{34}N_2O_2PAu$: C, 54.40; H, 4.85; N, 3.96. Found: C, 54.37; H, 4.95; N, 4.02.

X-ray structure analysis

All measurements for **U6AuCNPh** were performed with a Rigaku R-AXIS RAPID diffractometer by using graphite-monochromated Mo-Kα radiation. All measurements for **U6AuPPh$_3$** were performed with a Rigaku R-AXIS RAPID diffractometer by using filtered Mo-Kα radiation. The structures of **U6AuCNPh** and **U6AuPPh$_3$** were solved by direct methods[5] and expanded using Fourier techniques. All calculations were performed using the CrystalStructure crystallographic software package[6] except for the refinement, which was performed using SHELXL-97.[7] The non-hydrogen atoms were refined anisotropically. The H atoms involved in hydrogen bonding were located in electron density maps. The remainder of the H atoms were placed in idealized positions and allowed to ride with the C atoms to which each was bonded. Crystallographic details are given in Table 2. Selected bond distances and angles are shown in Table 3 and 4. Crystallographic data (excluding structure factors) for the structures reported in this paper have been deposited with the Cambridge Crystallographic Data Centre as supplementary publication no. CCDC-1026761 for **U6AuCNPh** and CCDC-1026762 for **U6AuPPh$_3$**. Copies of the data can be obtained free of charge on application to CCDC, 12 Union Road, Cambridge CB2 1EZ, UK [Fax: (internat.) +44-1223/336-033; E-mail: deposit@ccdc.cam.ac.uk].

Table 2. Crystallographic data for **U6AuCNPh** and **U6AuPPh$_3$**

	U6AuCNPh	**U6AuPPh$_3$**
Formula	$C_{21}H_{24}N_3O_2Au_1$	$C_{32}H_{34}N_2O_2P_1Au_1$
Molecular weight	541.41	706.57
Crystal system	Tetragonal	Monoclinic
Space group	$I4_1/a$ (No. 88)	$C2/c$ (No. 15)
a (Å)	35.091(3)	38.4526(14)
b (Å)		16.5099(4)
c (Å)	6.7679(6)	20.2551(7)
β (°)		114.7260(11)
V (Å^3)	8334.0(12)	11680.0(7)
Z	16	16
D_{calcd} (g cm^{-3})	1.745	1.607
μ (Mo Ka) (cm^{-1})	71.052	51.414
T (°C)	–150	–170
λ (Mo Kα) (Å)	0.71075	0.71075
$R1$[a]	0.062	0.060
$wR2$[b]	0.156	0.152

(a) $R1 = \Sigma||F_o| - |F_c|| / \Sigma|F_o|$. (b) $wR2 = [\Sigma w(F_o^2 - F_c^2)^2 / \Sigma w(F_o^2)^2]^{1/2}$.

Table 3. Selected bond distances (Å) for **U6AuCNPh** and **U6AuPPh$_3$**

	U6AuCNPh	**U6AuPPh$_3$**[a]	
Au(1)–C(15)	1.982(11)		
Au(1)–P(1)		2.2783(18)	2.2762(18)
Au(1)–C(14)	1.990(11)	1.998(8)	2.002(8)
P(1)–C(15)		1.818(10)	1.821(10)
P(1)–C(21)		1.811(8)	1.825(7)
P(1)–C(27)		1.812(7)	1.806(7)
O(1)–C(1)	1.242(14)	1.220(9)	1.22613)
O(2)–C(2)	1.215(15)	1.230(8)	1.223(10)
N(1)–C(1)	1.361(14)	1.392(10)	1.364(13)
N(1)–C(4)	1.415(14)	1.391(10)	1.356(12)
N(2)–C(1)	1.356(16)	1.381(9)	1.333(12)
N(2)–C(2)	1.420(15)	1.393(9)	1.360(10)
N(3)–C(15)	1.134(14)		
N(3)–C(16)	1.404(13)		
C(2)–C(3)	1.425(15)	1.427(10)	1.433(11)
C(3)–C(4)	1.350(16)	1.364(10)	1.356(11)
C(4)–C(13)	1.421(14)	1.436(11)	1.410(10)
C(13)–C(14)	1.198(14)	1.205(12)	1.214(11)

(a) Two independent molecules exist in an asymmetric unit.

Table 4. Selected bond angles (°) for **U6AuCNPh** and **U6AuPPh$_3$**

	U6AuCNPh	**U6AuPPh$_3$**[a]	
C(14)–Au(1)–C(15)	176.0(4)		
P(1)–Au(1)–C(14)		176.3(3)	176.2(2)
Au(1)–C(15)–N(3)	176.4(9)		
Au(1)–P(1)–C(15)		111.5(2)	111.5(3)
Au(1)–P(1)–C(21)		116.2(3)	116.6(3)
Au(1)–P(1)–C(27)		110.8(2)	112.4(2)
Au(1)–C(14)–C(13)	173.6(9)	177.6(8)	174.4(9)
O(1)–C(1)–N(1)	123.1(11)	122.9(7)	121.8(9)
O(1)–C(1)–N(2)	120.7(10)	122.3(7)	121.5(9)
O(2)–C(2)–N(2)	120.2(10)	119.5(6)	119.3(7)
O(2)–C(2)–C(3)	126.0(11)	125.9(7)	125.6(8)
N(1)–C(1)–N(2)	116.1(10)	114.8(6)	116.7(9)
N(1)–C(4)–C(3)	119.9(9)	121.2(7)	118.5(7)
N(1)–C(4)–C(13)	117.9(9)	116.3(6)	119.4(7)
N(2)–C(2)–N(3)	113.8(10)	125.9(7)	115.1(7)
C(1)–N(1)–C(4)	122.0(9)	121.6(6)	123.0(9)
C(1)–N(2)–C(2)	126.4(9)	126.7(6)	125.5(7)
C(2)–C(3)–C(4)	121.5(10)	121.0(7)	120.7(7)
C(3)–C(4)–C(13)	122.2(10)	122.5(7)	121.9(7)
C(4)–C(13)–C(14)	172.7(11)	178.1(12)	174.7(11)
C(15)–N(3)–C(16)	176.4(11)		

(a) Two independent molecules exist in an asymmetric unit.

2-5. References

1. For recent reviews, see: (a) H. Schmidbaur, *Chem. Soc. Rev.* 1995, **24** 391; (b) P. Pyykkő, *Chem. Rev.* 1997, **97**, 597; (c) M. J. Katz, K. Sakai and D. B. Leznoff, *Chem. Soc. Rev.* 2008, **37**, 1884; (d) I. Ott, *Coord. Chem. Rev.* 2009, **253,** 1670; (e) H. Schmidbaur and A. Schier, *Chem. Soc. Rev.* 2012, **41**, 370.
2. T. Moriuchi, S. Noguchi, Y. Sakamoto and T. Hirao, *J. Organomet. Chem.*, 2011, **696**, 1089.
3. A. S. K. Hashmi, T. Hengst, C. Lothschütz and F. Rominger, *Adv. Synth. Catal*. 2010, **352**, 1315.
4. R. Usón, A. Laguna, J. Vicente, J. García, B. Bergareche and P. Brun, *Inorg. Chim. Acta* 1978, **28**, 237.
5. A. Altomare, M. C. Burla, M. Camalli, G. L. Cascarano, C. Giacovazzo, A. Guagliardi, A. G. G. Moliterni, G. Polidori and R. Spagna, *J. Appl. Cryst.*, 1999, **32**, 115.
6. CrystalStructure 4.0: Crystal Structure Analysis Package, Rigaku Corporation (2000-2010). Tokyo 196-8666, Japan.
7. G. M. Sheldrick, *Acta Crystallogr., Sec. A* 2008, **64**, 112.

Chapter 3. Induced Au(I)-Au(I) interaction of dinuclear organogold(I) complexes with diphosphine ligands and uracil moieties

3-1. Introduction

As mentioned in the chapter 2, Au(I)-Au(I) interaction in the gold(I) complexes is influenced by steric structure of ancillary ligands. The dinuclear gold(I) complex with a bridging ligand is conceived to be a useful approach for the design of well-designed aggregates.[1] Arrangement of metal centers in the same side of the ligand is expected by using the semirigid bridging diphosphine ligand. Xantphos and (*R*)-BINAP were focused on as the bridging diphosphine ligand. The advantage in the use of Xantphos and (*R*)-BINAP derived from their semirigid backbone to arrange the phosphorus atoms on the same side. From these points of view, I herein report designs and syntheses of the dinuclear organogold(I)-uracil conjugates with the bridging diphosphine ligands in order to control the arrangement of Au(I) centers and self-assembly properties of the uracil moieties.

3-2. Result and discussion

The dinuclear organogold(I)-uracil conjugates with the bridging diphosphine ligands were synthesized by the introduction of Xantphos and (*R*)-BINAP to cause an intramolecular aurophilic Au(I)-Au(I) interaction. The dinuclear organogold(I)-uracil conjugates **(U6Au)$_2$(*μ*-Xantphos)**, **(U5Au)$_2$(*μ*-Xantphos)** and **(U6Au)$_2$(*μ*-*R*-BINAP)** were obtained by the reaction of 6-ethynyl-1-octyluracil or 5-ethynyl-1-octyluracil with (ClAu)$_2$(*μ*-diphosphine) (diphosphine = Xantphos or (*R*)-BINAP), which were produced by the treatment of chloro(tetrahydrothiophene)gold(I) [ClAu(tht)] with the corresponding diphosphine *in situ*, in the presence of sodium bis(trimethylsilyl)amide (Scheme 1). Thus-obtained dinuclear organogold(I)-uracil conjugates were fully confirmed by ^{1}H NMR, ^{13}C NMR, ^{31}P NMR, IR, HRMS, and elemental analysis. In the ^{1}H NMR spectra, the signal for the ethynyl proton of the uracil derivatives disappeared and the upfield shift of the uracil proton was observed after the introduction of the Au(I) center. The ^{31}P NMR spectra of **(U6Au)$_2$(*μ*-Xantphos)**, **(U5Au)$_2$(*μ*-Xantphos)** and **(U6Au)$_2$(*μ*-*R*-BINAP)** exhibited only one kind of resonance at around 30 ppm in CD_2Cl_2, suggestng that two phosphorus atoms of the dinuclear organogold(I)-uracil conjugates are equivalent in NMR time scale.

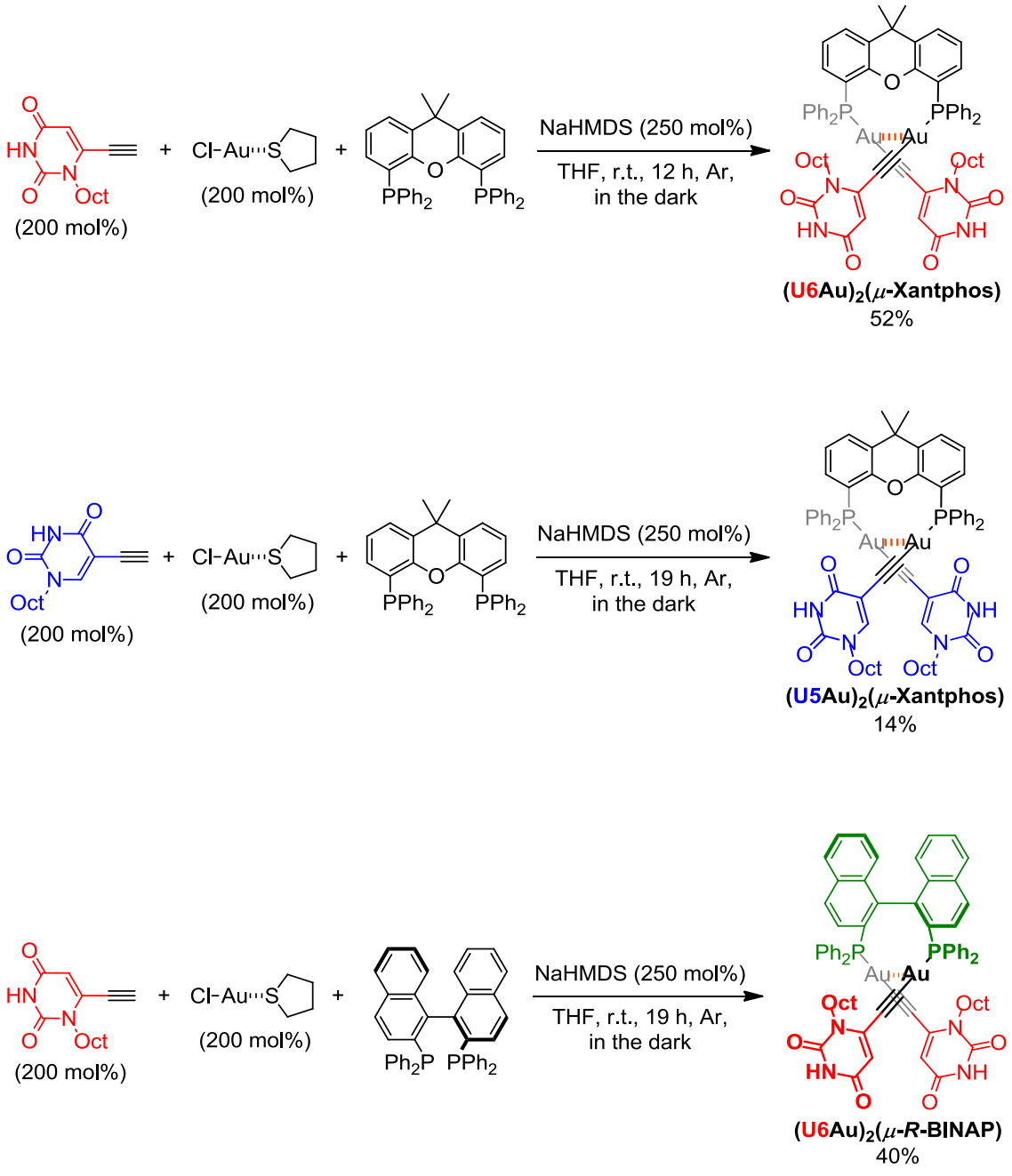
(200 mol%)
Cl-Au
(200 mol%)
NaHMDS (250 mol%)
THF, r.t., 12 h, Ar,
in the dark
(U6Au)2(μ-Xantphos)
52%
(200 mol%)
(200 mol%)
NaHMDS (250 mol%)
THF, r.t., 19 h, Ar,
in the dark
(U5Au)2(μ-Xantphos)
14%
(200 mol%)
(200 mol%)
NaHMDS (250 mol%)
THF, r.t., 19 h, Ar,
in the dark
(U6Au)2(μ-R-BINAP)
40%

Scheme 1.

X-ray crystallographic analyses were performed in order to elucidate the coordination environment of Au(I) centers and self-assembly properties of the dinuclear organogold(I)-uracil conjugates. Diffraction-quality single crystals of **(U6Au)$_2$(μ-Xantphos)** and **(U5Au)$_2$(μ-Xantphos)** were prepared by diffusion of methanol into dichloromethane solution of **(U6Au)$_2$(μ-Xantphos)** and diffusion of hexane into dichloromethane solution of **(U5Au)$_2$(μ-Xantphos)**. The dinuclear structure of **(U6Au)$_2$(μ-Xantphos)** bearing 6-ethynyl-1-octyluracil moiety was determined by single-crystal X-ray structure determination (Figure 1). The crystal structure showed a linear coordination geometry of the Au(I) centers bridged by Xantphos ligand. It is a noteworthy that an intramolecular aurophilic Au(I)-Au(I) interaction was observed with Au(1)-Au(2) distance of 2.9994(8) Å. The semirigid xanthene backbone was found to facilitate the arrangement of the phosphorus atoms on the same side to induce intramolecular Au(I)-Au(I) interaction. The conformational enantiomers based on the torsional twist about the Au(I)-Au(I) axis are possible in the dinuclear gold(I)-uracil conjugates (Figure 2). The dinuclear organogold(I) complex **(U6Au)$_2$(μ-Xantphos)** crystallized in the space group *P*-1 with *R*- and *S*-enantiomers based on the Au(I)-Au(I) axis in the unit cell (Figures 1a). The Au(I)-Au(I) interaction was found to induce the deviation from the linearity of the coordination structures of the Au centers with P-Au-C angles of 168.1(4)° and 174.5(5)°. The torsion angle of P(1)-Au(1)-Au(2)-P(2) of 82° indicates that the P-Au-C moieties are almost perpendicular to each other. Furthermore, the heterochiral hydrogen-bonded assembly was formed by connecting the each enantiomer alternately through intermolecular hydrogen bonds between the uracil moieties (Figure 1b and Table 1). There are two types of hydrogen bonding pattern in the heterochiral hydrogen bonded assembly, wherein one uracil moiety is linked by the

hydrogen bonded bridges of methanol solvent molecules and another uracil moiety is linked by hydrogen-bonded to the uracil moiety of another molecule directly (Figure 1b).

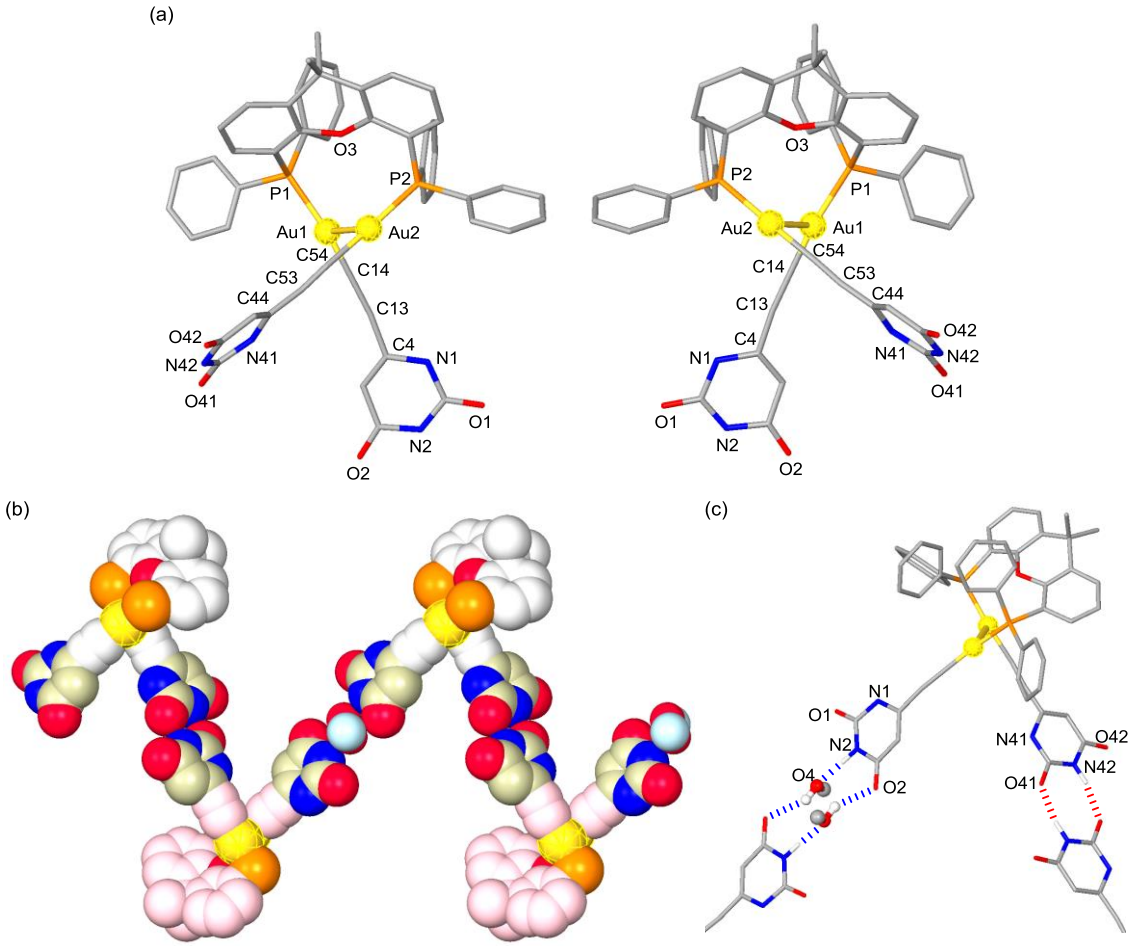

Figure 1. (a) Molecular structures of the *R*- and *S*-enantiomers of the dinuclear organogold(I)-uracil conjugates **(U6Au)$_2$(*μ*-Xantphos)**, (b) the heterochiral hydrogen-bonded assembly through intermolecular hydrogen bonds between the uracil moieties of **(U6Au)$_2$(*μ*-Xantphos)** and (c) a part of the crystal structure showing two types of the hydrogen bonding pattern in the heterochiral hydrogen-bonded assembly (hydrogen atoms and octyl moieties are omitted for clarity).

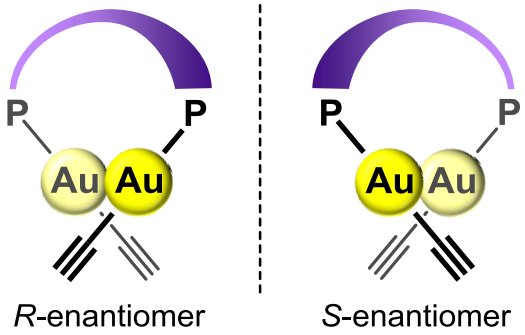

Figure 2. Enantiomorphous conformations of the dinuclear organogold(I)-uracil conjugates with the bridging diphosphine ligands by . The enantiomorphs are related by the mirror plane.

Table 1. Intermolecular hydrogen bonds for **(U6Au)$_2$(μ-Xantphos)**, **U5Au)$_2$(μ-Xantphos)** and **(U6Au)$_2$(μ-R-BINAP)**

Compounds	Donor	Acceptor	D•••A (Å)	D–H•••A (°)
(U6Au)$_2$(μ-Xantphos)	O(4)[a]	O(2)[b]	2.73(2)	147(10)
	N(2)	O(4)[a]	2.78(2)	172(5)
	N(42)	O(41)[c]	2.798(15)	167(4)
(U5Au)$_2$(μ-Xantphos)	N(2)	O(42)[d]	2.816(13)	166(4)
	N(42)	O(1)[e]	2.924(13)	169(3)
(U6Au)$_2$(μ-R-BINAP)	N(2)	O(41)[f]	2.816(17)	158(4)
	N(42)	O(2)[g]	2.789(18)	176(4)

(a) Oxygen atom of methanol. (b) –X+2, –Y+1, –Z+2. (c) –X+2, –Y+1, –Z+1. (d) X, –Y, Z+1/2. (e) X, –Y, Z+1/2–1. (f) –X+2, Y+1/2–1, –Z+1/2. (g) –X+2, Y+1/2, –Z+1/2.

In the crystal structure of **(U5Au)$_2$(μ-Xantphos)** composed of 5-ethynyl-1-octyluracil, wherein the direction of hydrogen bonding sites of the uracil moieties is different from **(U6Au)$_2$(μ-Xantphos)**, an intramolecular aurophilic Au(I)-Au(I) interaction with Au(1)-Au(2) distance of 2.9287(9) Å was also determined by single-crystal X-ray structure determination. *R*- and *S*-enantiomers based on Au(I)-Au(I) axis in **(U5Au)$_2$(μ-Xantphos)** were present as depicted in Figure 3a. The distortion of the linear coordination geometry of the Au centers based on the Au(I)-Au(I) interaction was also observed, resulting in P-Au-C angles of 166.9(3)° and 176.1(3)°. Compared with **(U6Au)$_2$(μ-Xantphos)**, the P(1)-Au(1)-Au(2)-P(2) torsion angle of 78.96(10)° was slightly small. The Au-C bond of **(U5Au)$_2$(μ-Xantphos)** was a little shorter than that of **(U6Au)$_2$(μ-Xantphos)**. The position of the introduced ethynyl moiety of the uracil is likely to influence the electronic environment of the Au centers. Interestingly, a homochiral π stacked dimer was formed through π–π interactions between the uracil moieties of each enantiomer (Figure 3b). Furthermore, each homochiral π stacked dimer was linked alternately for formation of the hydrogen-bonded assembly through intermolecular hydrogen bonds between the uracil moieties (Figure 3c and Table 1). The direction of hydrogen bonding sites were found to affect the self-assembly patterns.

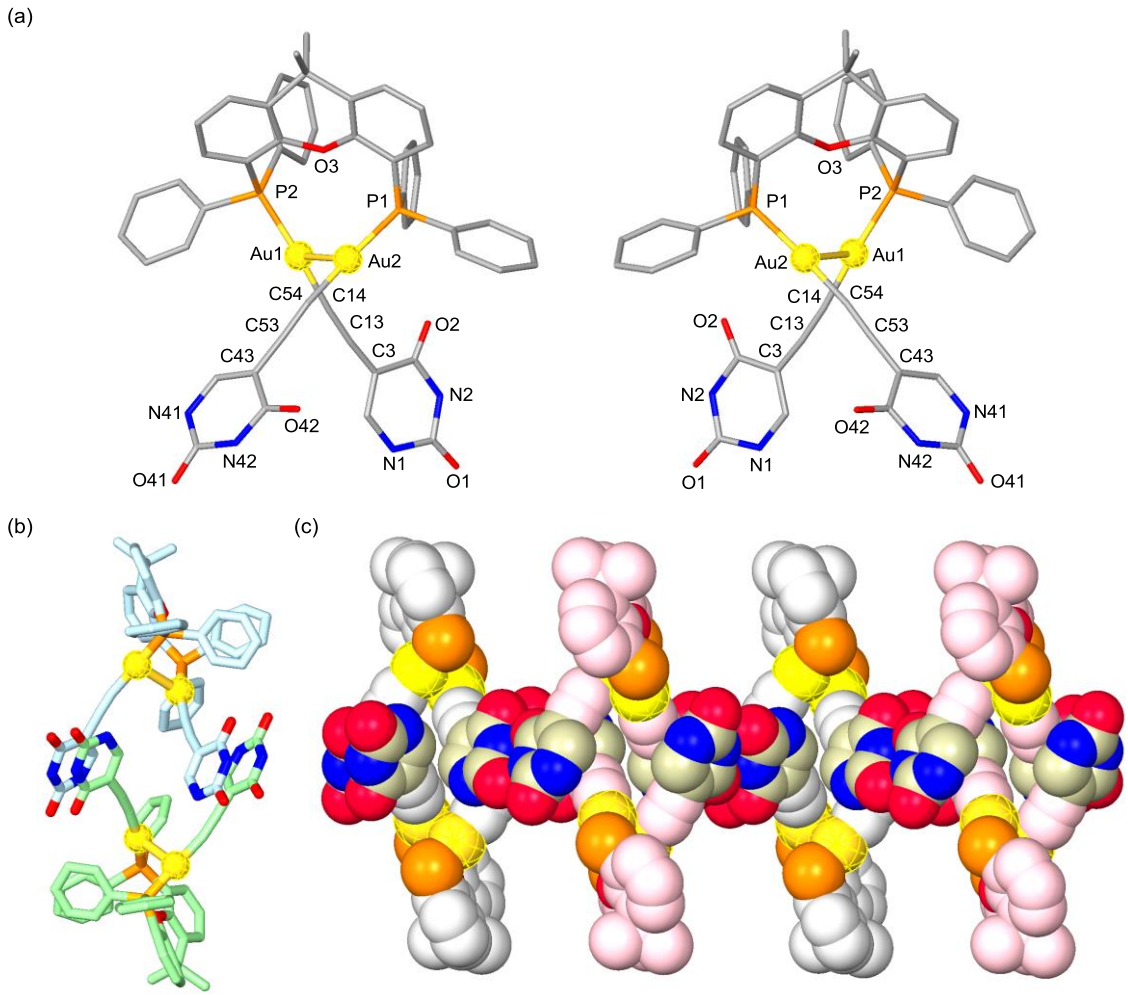

Figure 3. (a) Molecular structures of the *R*- and *S*-enantiomers, (b) the homochiral π stacked dimer, and (c) the heterochiral hydrogen-bonded assembly through intermolecular hydrogen bonds between the uracil moieties of the dinuclear organogold(I)-uracil conjugate **(U5Au)$_2$(*μ*-Xantphos)** (hydrogen atoms and octyl moieties are omitted for clarity).

Based on the above-mentioned interesting results, we launched on the chirality induction in Au(I)-Au(I) axis by using the bridging diphosphine ligand with axial chirality. Diffraction-quality single crystal of **(U6Au)$_2$(*μ*-*R*-BINAP)** was prepared by diffusion of hexane into chloroform solution of **(U6Au)$_2$(*μ*-*R*-BINAP)**. The dinuclear organogold(I)-uracil conjugate **(U6Au)$_2$(*μ*-*R*-BINAP)** crystallized in the space group $P2_12_12_1$; the molecular structure exhibited an intramolecular Au(I)-Au(I) interaction based on the aurophilic interaction (Figure 4). The deviation from the linear coordination structure of the Au centers with P-Au-C angles of 172.2(5)° and 176.5(4)° based on the Au(I)-Au(I) interaction was also observed. The crystal structure of **(U6Au)$_2$(*μ*-*R*-BINAP)** showed the P(1)-Au(1)-Au(2)-P(2) torsion angle of 71.97(8)°, which is smaller than that of the gold(I)-uracil conjugates with Xantphos probably due to the difference for rigidity of the diphosphine frameworks. Gratifyingly, **(U6Au)$_2$(*μ*-*R*-BINAP)** assumed *R*,*R*-configuration through the chirality induction in Au(I)-Au(I) axis by the axial chirality of BINAP moiety as shown in Figure 4a. Although Au(I)-Au(I) aurophilic interactions have been researched by using the bridging diphosphine ligand,[1] to the best of our knowledge, the chirality induction in Au(I)-Au(I) axis has not been reported so far. In the crystal packing, a left-handed helical molecular arrangement was found to form by assembling of each molecule through intermolecular hydrogen bonds between the uracil moieties as shown in Figure 4b.

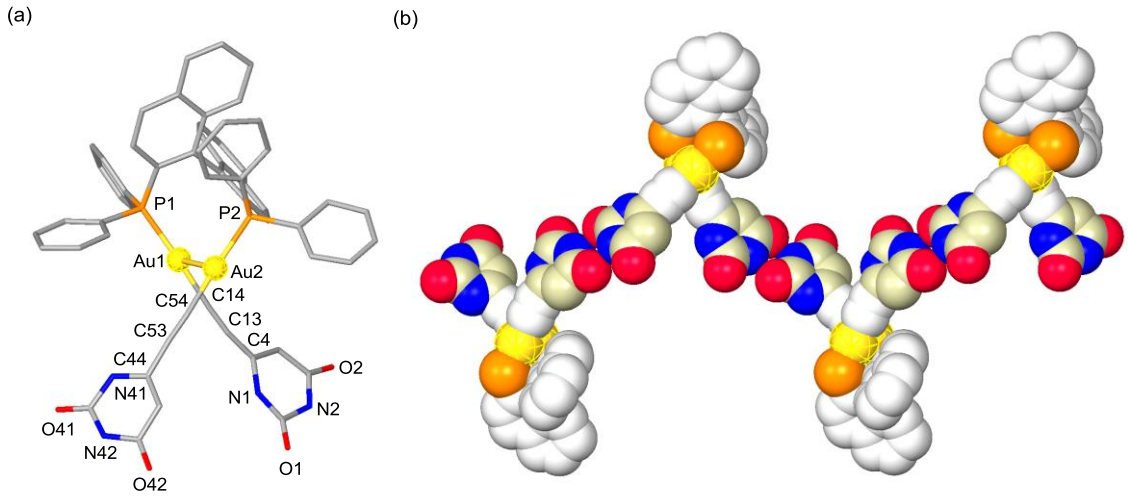

Figure 4. (a) Molecular structure of the *R*-enantiomer and (b) the homochiral hydrogen-bonded assembly through intermolecular hydrogen bonds between the uracil moieties of the dinuclear organogold(I)-uracil conjugate **(U6Au)$_2$(*μ*-*R*-BINAP)** (hydrogen atoms and octyl moieties are omitted for clarity).

3-3. Conclusions

In conclusion, the combination of the dinuclear organogold(I) complexes with a bridging diphosphine ligand as an organometallic compound and the uracil derivative as a nucleobase was established to afford the bioorganometallic conjugates. The single-crystal X-ray structure determination of the dinuclear organogold(I)-uracil conjugates was demonstrated to disclose the assembly properties of the gold(I) and the uracil moieties in a solid state. The semirigid bridging diphosphine ligand was found to play an important role in the arrangement of the phosphorus atoms on the same side and to support the induction of intramolecular aurophilic Au(I)-Au(I) interaction, wherein *R*- and *S*-enantiomers based on Au(I)-Au(I) axis exist. It should be noted that the chirality of Au(I)-Au(I) axis was induced by the utilization of (*R*)-BINAP as the bridging diphosphine ligand with axial chirality. Their strong tendency to self-assemble through intermolecular hydrogen bonds between the uracil moieties is Interesting feature of the dinuclear organogold(I)-uracil conjugate. These hydrogen bonding patterns were found to depend on the direction of hydrogen bonding sites.

3-4. Experimental section

General methods

All reagents and solvents were purchased from commercial sources and were further purified by the standard methods, if necessary. All manipulations were carried out under Ar. Infrared spectra were obtained with a JASCO FT/IR-6200 spectrometer. ^{1}H, ^{13}C, and ^{31}P NMR spectra were recorded on a JNM-ECS 400 (400, 100 and 160 MHz, respectively) spectrometer. For ^{1}H and ^{31}P NMR spectra, chemical shifts were determined by using of tetramethylsilane and 85% H_3PO_4 aq. as standard samples, respectively. Chemical shifts of ^{13}C NMR spectra were determined relative to the solvent residual peaks. Mass spectra were run on a JEOL JMS-700 mass spectrometer.

6-Ethynyl-1-octyluracil,[2] 5-ethynyl-1-octyluracil,[3] and chloro(tetrahydrothiophene)gold(I) [ClAu(tht)][4] were prepared by the literature methods.

Synthesis of the dinuclear organogold(I)-uracil conjugate $(U6Au)_2(\mu$-Xantphos)

A mixture of Xantphos (116 mg, 0.20 mmol), chloro(tetrahydrothiophene)gold(I) (128 mg, 0.40 mmol), and 6-ethynyl-1-octyluracil (**1**) (100 mg, 0.40 mmol) was stirred in THF (20 mL) at room temperature for 10 minutes under Ar. To the solution was added sodium bis(trimethylsilyl)amide (93 mg, 0.51 mmol) and the resulting solution was stirred at room temperature under Ar for 12 h. The mixture was diluted with dichloromethane, washed with water, brine, and then dried over Na_2SO_4. The solvent was evaporated and the residue was washed with ethyl acetate. The crude product was purified by recrystallization from dichloromethane and methanol to afford the desired dinuclear organogold(I)-uracil conjugate

(U6Au)$_2$(μ-Xantphos) (153 mg, 0.10 mmol) as a colorless crystal.

(U6Au)$_2$(μ-Xantphos): yield 52%; IR (KBr) 3172, 3047, 2925, 2854, 2119, 1677, 1579, 1435, 1403, 1363, 1227 cm^{-1}; ^{1}H NMR (400 MHz, CD_2Cl_2, 5.0 x 10^{-3} M): δ 8.22 (br, 2H), 7.69 (dd, 2H, J = 7.8, 1.4 Hz), 7.48-7.44 (m, 4H), 7.34-7.23 (m, 16H), 7.11 (td, 2H, J = 7.8 Hz, $^4J_{H\text{-}P}$ = 1.2 Hz), 6.48 (ddd, 2H, J = 7.8, 1.4 Hz, $^3J_{H\text{-}P}$ = 12.1 Hz), 5.67 (s, 2H), 4.01 (t, 4H, J = 7.2 Hz), 1.69 (s, 6H), 1.67-1.60 (m, 4H), 1.29-1.12 (m, 20H), 0.81 (t, 6H, J = 6.8 Hz); ^{13}C NMR (100 MHz, CD_2Cl_2, 5.0 x 10^{-3} M): 163, 153 (d, $^2J_{C\text{-}P}$ = 4.0 Hz), 151.3, 150.2 (d, $^2J_{C\text{-}P}$ = 140.9 Hz),140.8, 134.6 (d, $^2J_{C\text{-}P}$ = 14.9 Hz), 133.4, 132, 130, 129.8 (d, $^1J_{C\text{-}P}$ = 51.8 Hz), 129.5 (d, $^3J_{C\text{-}P}$ = 12 Hz), 124.9 (d, $^3J_{C\text{-}P}$ = 9.1 Hz), 117 (d, $^1J_{C\text{-}P}$ = 52.2 Hz), 104.8, 95.5 (d, $^3J_{C\text{-}P}$ = 26.8 Hz), 46.6, 35.1, 32.2, 31.6, 29.8, 29.6, 29.2, 27.1, 23, 14.2 ppm; ^{31}P NMR (160 MHz, CD_2Cl_2, 5.0 x 10^{-3} M): 31.2 ppm; HRMS (FAB) *m/z* Calcd. for $C_{67}H_{71}N_4O_5P_2Au_2$ (M + H$^+$), 1467.4225; Found, 1467.4215; Anal. Calcd. for $C_{67}H_{70}N_4O_5P_2Au_2$: C, 54.85; H, 4.81; N, 3.82. Found: C, 54.85; H, 4.94; N, 3.82.

Synthesis of the dinuclear organogold(I)-uracil conjugate (U5Au)$_2$(μ-Xantphos)

A mixture of Xantphos (58 mg, 0.10 mmol), chloro(tetrahydrothiophene)gold(I) (64 mg, 0.20 mmol), and 5-ethynyl-1-octyluracil (**2**) (50 mg, 0.40 mmol) was stirred in THF (10 mL) at room temperature for 10 minutes under Ar. To the solution was added sodium bis(trimethylsilyl)amide (47 mg, 0.25 mmol) and the resulting solution was stirred at room temperature under Ar for 19 h. The mixture was diluted with dichloromethane, washed with water, brine, and then dried over Na_2SO_4. The solvent was evaporated and purification of the crude product by preparative thin-layer chromatography using dichloromethane/methanol (93:7 v/v) as

mobile phase gave the desired dinuclear organogold(I)-uracil conjugate **(U5Au)$_2$(μ-Xantphos)** (20 mg, 0.014 mmol). Recrystallization from dichloromethane and hexane produced a yellow crystal.

(U5Au)$_2$(μ-Xantphos): yield 14%; IR (KBr) 3178, 3053, 2925, 2854, 2116, 1682, 1435, 1403, 1343, 1221 cm^{-1}; ^{1}H NMR (400 MHz, CD_2Cl_2, 5.0 x 10^{-3} M): δ 8.15 (br, 2H), 7.66 (d, 2H, J = 7.7 Hz), 7.45-7.41 (m, 6H), 7.36-7.27 (m, 16H), 7.09 (t, 2H, J = 7.7 Hz), 6.49 (dd, 2H, J = 7.7 Hz, $^2J_{H\text{-}P}$ = 11.4 Hz), 3.66 (t, 4H, J = 7.3 Hz), 1.69-1.60 (m, 10H), 1.33-1.22 (m, 20H), 0.87 (t, 6H, J = 6.8 Hz); ^{13}C NMR (100 MHz, CD_2Cl_2, 5.0 x 10^{-3} M): 162.8, 153.1 (d, $^2J_{C\text{-}P}$ = 2.0 Hz), 151.1, 146.1, 137.5 (d, $^2J_{C\text{-}P}$ = 141.6 Hz), 134.8 (d, $^2J_{C\text{-}P}$ = 14.5 Hz), 133.3, 132, 131.5, 130.7(d, $^1J_{C\text{-}P}$ = 55.8 Hz), 129.6, 129.3 (d, $^3J_{C\text{-}P}$ =11.4 Hz), 124.6 (d, $^3J_{C\text{-}P}$ = 8.1 Hz) 117.8 (d, $^1J_{C\text{-}P}$ = 50.5 Hz), 102.3, 94.6 (d, $^3J_{C\text{-}P}$ = 28.6 Hz), 49.1, 35, 32.1, 31.4, 29.5, 29.4, 26.7, 23, 14.2 ppm; ^{31}P NMR (160 MHz, CD_2Cl_2, 5.0 x 10^{-3} M): 31.8 ppm; HRMS (FAB) *m/z* Calcd. for $C_{67}H_{71}N_4O_5P_2Au_2$ (M + H^+), 1467.4225; Found, 1467.4171.

Synthesis of the dinuclear organogold(I)-uracil conjugate (U6Au)$_2$(μ-*R*-BINAP)

A mixture of (*R*)-BINAP (125 mg, 0.20 mmol), chloro(tetrahydrothiophene)gold(I) (128 mg, 0.40 mmol), and 6-ethynyl-1-octyluracil (**1**) (99 mg, 0.20 mmol) was stirred in THF (20 mL) at room temperature for 20 minutes under Ar. To the solution was added sodium bis(trimethylsilyl)amide (93 mg, 0.51 mmol) and the resulting solution was stirred at room temperature under Ar for 19 h. The mixture was diluted with dichloromethane, washed with water, brine, and then dried over Na_2SO_4. The solvent was evaporated and purification of the crude product by preparative thin-layer chromatography using dichloromethane/methanol (93:7 v/v) as

mobile phase gave the desired dinuclear organogold(I)-uracil conjugate **(U6Au)$_2$(μ-*R*-BINAP)** (121 mg, 0.080 mmol). Recrystallization from chloroform, diethyl ether and hexane produced a pale yellow crystal.

(U6Au)$_2$(μ-*R*-BINAP): yield 40%; IR (KBr) 3165, 3049, 2925, 2853, 2118, 1683, 1582, 1456, 1407, 1367 cm^{-1}; ^{1}H NMR (400 MHz, CD_2Cl_2, 1.0 x 10^{-2} M): δ 8.69 (br, 2H), 8.11 (d, 2H, J = 8.8 Hz), 7.93 (d, 2H, J = 8.2 Hz), 7.76-7.71 (m, 4H), 7.59 (t, 2H, J = 8.8 Hz, $^3J_{H\text{-}P}$ = 8.8 Hz), 7.49-7.36 (m, 10H), 7.25-7.17 (m, 8H), 6.87-6.83 (m, 2H), 6.60 (d, 2H, J = 8.5 Hz), 5.65 (s, 2H), 4.01-3.90 (m, 4H), 1.68-1.60 (m, 4H), 1.34-1.14 (m, 20H), 0.83 (t, 6H, J = 6.8 Hz); ^{13}C NMR (100 MHz, CD_2Cl_2, 1.0 x 10^{-2} M): 163.3, 152.1 (d, $^2J_{C\text{-}P}$ = 141.9 Hz), 151.4, 143.3 (dd, $^2J_{C\text{-}P}$ = 16 Hz, $^3J_{C\text{-}P}$ = 7.2 Hz), 140.7 (d, $^4J_{C\text{-}P}$ = 2.6 Hz), 135.3 (d, $^2J_{C\text{-}P}$ = 14 Hz), 135, 134.8 (d, $^2J_{C\text{-}P}$ = 14.6 Hz), 134.1 (d, $^3J_{C\text{-}P}$ = 10 Hz), 131.8, 130.5 (d, $^3J_{C\text{-}P}$ = 4.8 Hz), 130.4 (d, $^1J_{C\text{-}P}$ = 56.6 Hz), 130.2 (d, $^2J_{C\text{-}P}$ = 8.4 Hz), 129.5 (d, $^3J_{C\text{-}P}$ = 11.5 Hz), 129.3 (d, $^3J_{C\text{-}P}$ = 11.7 Hz), 128.9 (d, $^1J_{C\text{-}P}$ = 56.6 Hz), 128.8, 128.6, 128.2 (d, $^1J_{C\text{-}P}$ = 56.2 Hz), 127.4, 127.3, 105.1, 93.2 (d, $^3J_{C\text{-}P}$ = 25.9 Hz), 46.6, 32.2, 29.8, 29.7, 29.1, 27.1, 23, 14.2 ppm; ^{31}P NMR (160 MHz, CD_2Cl_2, 1.0 x 10^{-2} M): 33.5 ppm; HRMS (FAB) *m/z* Calcd. for $C_{72}H_{71}N_4O_4P_2Au_2$ (M + H$^+$), 1511.4276; Found, 1511.4257; Anal. Calcd. for $C_{72}H_{70}N_4O_4P_2Au_2$•$CHCl_3$: C, 53.77; H, 4.39; N, 3.44. Found: C, 53.78; H, 4.45; N, 3.42.

X-ray structure analysis

All measurements for **(U6Au)$_2$(μ-Xantphos)**, **(U5Au)$_2$(μ-Xantphos)**, and **(U6Au)$_2$(μ-*R*-BINAP)** were made on a Rigaku R-AXIS RAPID diffractometer using graphite monochromated MoKα radiation. The structures of **(U6Au)$_2$(μ-Xantphos)**, **(U5Au)$_2$(μ-Xantphos)**, and **(U6Au)$_2$(μ-*R*-BINAP)** were solved by direct methods[5] and expanded using Fourier techniques. All calculations were performed using the CrystalStructure crystallographic software package[6] except for the refinement, which was performed using SHELXL-97.[7] The non-hydrogen atoms were refined anisotropically. The H atoms involved in hydrogen bonding were located in electron density maps. The remainder of the H atoms were placed in idealized positions and allowed to ride with the C atoms to which each was bonded. Crystallographic details are given in Table 2. Selected bond distances and angles are reported in Table 3. Crystallographic data (excluding structure factors) for the structures reported in this paper have been deposited with the Cambridge Crystallographic Data Centre as supplementary publication no. CCDC-1033826 for **(U6Au)$_2$(μ-Xantphos)**, CCDC-1033825 for **(U5Au)$_2$(μ-Xantphos)** and CCDC-1033824 for **(U6Au)$_2$(μ-*R*-BINAP)**. Copies of the data can be obtained free of charge on application to CCDC, 12 Union Road, Cambridge CB2 1EZ, UK [Fax: (internat.) +44-1223/336-033; E-mail: deposit@ccdc.cam.ac.uk].

Table 2. Crystallographic data for **(U6Au)$_2$(μ-Xantphos)**, **(U5Au)$_2$(μ-Xantphos)** and **(U6Au)$_2$(μ-*R*-BINAP)**

	(U6Au)$_2$(μ-Xantphos)	**(U5Au)$_2$(μ-Xantphos)**	**(U6Au)$_2$(μ-*R*-BINAP)**
Formula	$C_{67}H_{70}N_4O_5P_2Au_2$ ·CH_2Cl_2 ·CH_3OH	$C_{67}H_{70}N_4O_5P_2Au_2$ ·CH_2Cl_2	$C_{72}H_{70}N_4O_4P_2Au_2$ ·$CHCl_3$
Molecular weight	1584.17	1552.13	1630.63
Crystal system	Triclinic	Monoclinic	Orthorhombic
Space group	*P*–1 (No. 2)	*C*2/*c* (No. 15)	$P2_12_12_1$ (No. 19)
a (Å)	10.6798(6)	30.3688(18)	11.0678(16)
b (Å)	14.2920(7)	26.6704(15)	23.228(4)
c (Å)	22.3083(13)	21.7986(12)	27.246(4)
α (°)	97.4663(16)		
β (°)	90.7906(16)	109.0564(16)	
γ (°)	91.1556(14)		
V (Å^3)	3375.0(3)	16688.2(16)	7004.5(18)
Z	2	8	4
D_{calcd} (g cm^{-3})	1.559	1.235	1.546
μ (Mo Kα) (cm^{-1})	45.360	36.672	44.086
T (°C)	4.0	4.0	–150
λ (Mo Kα) (Å)	0.71075	0.71075	0.71075
*R*1[a]	0.083	0.054	0.078
*wR*2[b]	0.232	0.179	0.211

(a) $R1 = \Sigma||F_o| - |F_c|| / \Sigma|F_o|$. (b) $wR2 = [\Sigma w(F_o^2 - F_c^2)^2 / \Sigma w(F_o^2)^2]^{1/2}$.

Table 3. Selected bond distances (Å) and angles (°) for **(U6Au)$_2$(μ-Xantphos)**, **(U5Au)$_2$(μ-Xantphos)** and **(U6Au)$_2$(μ-*R*-BINAP)**

	(U6Au)$_2$(μ-Xantphos)	**(U5Au)$_2$(μ-Xantphos)**	**(U6Au)$_2$(μ-*R*-BINAP)**
Bond distances (Å)			
Au(1)–Au(2)	2.9994(8)	2.9286(5)	3.0021(9)
Au(1)–P(1)	2.283(4)	2.281(3)	2.281(4)
Au(2)–P(2)	2.275(3)	2.253(4)	2.290(4)
Au(1)–C(14)	2.009(14)	1.976(10)	2.066(14)
Au(2)–C(54)	2.002(17)	1.926(11)	2.003(17)
C(13)–C(14)	1.16(2)	1.230(13)	1.14(2)
C(53)–C(54)	1.18(2)	1.188(17)	1.16(2)
Bond angles (°)			
P(1)–Au(1)–C(14)	168.1(4)	166.9(3)	172.2(5)
P(2)–Au(2)–C(54)	174.5(5)	176.1(3)	176.5(4)
Au(1)–C(14)–C(13)	180.0(13)	175.1(11)	175.8(14)
Au(2)–C(54)–C(53)	173.1(16)	170.5(8)	175.6(14)
C(4)–C(13)–C(14)	173.3(17)		168.7(18)
C(44)–C(53)–C(54)	173(2)		175.3(18)
C(3)–C(13)–C(14)		171.6(13)	
C(43)–C(53)–C(54)		175.9(10)	

3-5. References

1. For recent reviews, see: (a) H. Schmidbaur, *Chem. Soc. Rev.* 1995, **24** 391; (b) P. Pyykkő, *Chem. Rev.* 1997, **97**, 597; (c) M. J. Katz, K. Sakai and D. B. Leznoff, *Chem. Soc. Rev.* 2008, **37**, 1884; (d) I. Ott, *Coord. Chem. Rev.* 2009, **253,** 1670; (e) H. Schmidbaur and A. Schier, *Chem. Soc. Rev.* 2012, **41**, 370.
2. T. Moriuchi, S. Noguchi, Y. Sakamoto and T. Hirao, *J. Organomet. Chem.*, 2011, **696**, 1089.
3. M. Takase and M. Inouye, *J. Org. Chem.*, 2003, **68**, 1134.
4. R. Usón, A. Laguna, J. Vicente, J. García, B. Bergareche and P. Brun, *Inorg. Chim. Acta* 1978, **28**, 237.
5. A. Altomare, M. C. Burla, M. Camalli, G. L. Cascarano, C. Giacovazzo, A. Guagliardi, A. G. G. Moliterni, G. Polidori and R. Spagna, *J. Appl. Cryst.*, 1999, **32**, 115.
6. CrystalStructure 4.0: Crystal Structure Analysis Package, Rigaku Corporation (2000-2010). Tokyo 196-8666, Japan.
7. G. M. Sheldrick, *Acta Crystallogr., Sec. A* 2008, **64**, 112.

Conclusion

In this dissertation, the synthesis of bioorganometallic compounds combined the organoplatinum(II) and organogold(I) complexes with the uracil and appearance of metal-metal interaction in the organometal-uracil conjugates is described. The structural characteristics and assembly properties of the organometal-uracil conjugates were determined by single-crystal X-ray structure determination, absorption and emission spectra and NMR measurement. Noncovalent bonds such as the hydrogen bonding and π–π interaction found to play an important role in aggregation of metal moieties and introduction of metal-metal interaction. These organometal-nucleobase conjugates are considered to have potential as probes, catalyst and pharmacy.

In chapter 1, the bioorganometallic platinum(II) compounds were synthesized by the reaction of the corresponding uracil derivative with the organoplatinum(II) compound. the platinum(II) complex bearing 6-ethynyl-1-octyluracil revealed the formation of the Pt(II)-Pt(II) interaction by supporting of intermolecular hydrogen bonding between the uracil moieties and π–π interaction between the phenylbipyridine ligands. Furthermore, controlled arrangement of organoplatinum(II) complexes bearing uracil moieties was achieved by changing molecular scaffolds, which having two 2,6-dihexamidopyridine moieties as a complementary hydrogen bonding site for the uracil moiety. The emission properties of the organoplatinum(II) compounds were tuned by the induced Pt(II)-Pt(II) and π–π interactions through the regulation of the aggregated structures.

In chapter 2, the conjugation of the gold(I) complex having a planar ligand or a bulky ligand with 6-ethynyl-1-octyluracil afforded the corresponding gold(I) complexes, respectively. The crystal structure of the gold(I)-urcil conjugate having the planar phenyl isocyanide ligand disclosed the formation of a head-to-tail dimer through the Au(I)-Au(I) and π–π interactions between the uracil and benzene moieties of phenyl isocyanide. Furthermore, each head-to-tail dimer was connected not only through the intermolecular hydrogen bonds of N-H•••O pattern between the uracil moieties but the weak hydrogen bonds of C-H•••O pattern between the uracil and benzene moieties of phenyl isocyanide. In contrast, the Au(I)-Au(I) interaction was not observed in a crystal structure of the gold(I)-uracil conjugate having the bulky triphenylphosphine ligand probably due to the steric hindrance of the bulky ligand

In chapter 3, the dinuclear gold(I)-uracil conjugates synthesized by the treatment of the dinuclear organogold(I) complexes with a bridging diphosphine ligand and the uracil derivative. The crystal structure of the dinuclear gold(I)-uracil conjugates with Xantphos as a bridging diphosphine ligand exhibited an intramolecular aurophilic Au(I)-Au(I) interaction. *R*- and *S*-enantiomers based on Au(I)-Au(I) axis are exist in the unit cell. By contrast, the utilization of (*R*)-BINAP as the bridging diphosphine ligand with axial chirality was performed to induce the chirality of Au(I)-Au(I) axis. The crystal structure of the dinuclear organogold(I) complex with (*R*)-BINAP confirmed the axial chirality in Au(I)-Au(I) axis to form *R,R*-enantiomer, wherein each molecule is arranged through intermolecular hydrogen bonds between the uracil moieties to form a helical molecular arrangement.

The structure characterization and assembly properties of the bioorganometallic compounds bearing the uracil moieties were demonstrated to be controlled by the molecular scaffolds or ancillary ligands. These results and findings provide a significant contribution for structural control of metal-metal interaction in bioorganometallic compounds.

List of Publication

(1) Design and controlled emission properties of bioorganometallic compounds composed of uracils and organoplatinum(II) moieties
Toshiyuki Moriuchi, Yuki Sakamoto, Shunichi Noguchi, Takashi Fujiwara, Shigehisa Akine, Tatsuya Nabeshima, and Toshikazu Hirao
Dalton Trans. **2012**, *41*, 8524-8531.

(2) Organogold(I)-Uracil Conjugates: Synthesis and Structural Characterization
Yuki Sakamoto, Toshiyuki Moriuchi, and Toshikazu Hirao
J. Organomet. Chem. in press.

(3) Dinuclear organogold(I) complexes bearing uracil moieties: chirality of Au(I)-Au(I) bond axis and self-assembling
Yuki Sakamoto, Toshiyuki Moriuchi, and Toshikazu Hirao
CrystEngComm, in press.

Supplementary Publications

(1) Synthesis and characterization of bioorganometallic conjugates composed of NCN-pincer platinum(II) complexes and uracil derivatives
Toshiyuki Moriuchi1, Syunichi Noguchi, Yuki Sakamoto, and Toshikazu Hirao
J. Organomet. Chem. **2011**, *690*, 1089-1095.

(2) $La(OTf)_3$-mediated self-organization of guanosine with an alkynyl-Au(I)PPh_3 moiety to induce Au(I)–Au(I) interactions
Xiangtai Meng, Toshiyuki Moriuchi1, Yuki Sakamoto, Masatoshi Kawahata, Kentaro Yamaguchi, and Toshikazu Hirao
RSC Adv. **2012**, *2*, 4359-4363.

(3) Molecular Structures of Dipeptide-Palladium(II) Conjugated Complexes
Toshiyuki Moriuchi, Kunihiro Morimoto, Yuki Sakamoto, and Toshikazu Hirao
Eur. J. Inorg. Chem. **2012**, 4669-4674.

(4) Self-Assembly Properties of NCN Pincer Palladium(II) Complexes Bearing a Uracil Moiety
Toshiyuki Moriuchi, Ryohei Ohata, Yuki Sakamoto, and Toshikazu Hirao
Eur. J. Inorg. Chem. **2014**, 4626-4631.

Acknowledgement

The author would like to express his sincerest gratitude to Professor Dr. Toshikazu Hirao, Department of Applied Chemistry, Graduate School of Engineering, Osaka University for his continuous guideline throughout this work and fruitful discussions.

The author would like to express deeply thanks to Professor Dr. Takashi Hayashi and Professor Dr. Hidehiro Sakurai, Department of Applied Chemistry, Graduate School of Engineering, Osaka University for reviewing this thesis and helpful comments.

The author would like to express his appreciation and gratitude to Dr. Toshiyuki Moriuchi, Department of Applied Chemistry, Graduate School of Engineering, Osaka University for his continuous guidance throughout these works, so many helpful suggestions, fruitful discussions, and hearty encouragement.

The author would like to express his special thanks to Dr. Toru Amaya, Department of Applied Chemistry, Graduate School of Engineering, Osaka University for his so many helpful advice and hearty encouragement.

The author would like to thank Professor Dr. Tatsuya Nabeshima, Graduate School of Pure and Applied Sciences, University of Tsukuba, and Professor Dr. Shigehisa Akine, Graduate School of Natural Science and Technology, Kanazawa University, for the measurement of association constants.

The author would like to express thanks to Professor Dr. Shinobu Itoh and Dr. Hideki Sugimoto, Department of Material and Life Science, Division of Advanced Science and Biotechnology, Graduate School of Engineering, Osaka University, for

performance of x-ray crystal structure analysis.

The author would like to express thanks to Dr. Nobuko Kanehisa, Department of Applied Chemistry, Graduate School of Engineering, Osaka University, for performance of x-ray crystal structure analysis and valuable comments.

The author would like to express thanks to Dr. Kyoko Inoue and Mr. Hiroshi Moriguchi, Laboratory for Instrumental Analysis, Graduate School of Engineering, Osaka University, for NMR experiments and measurements of HR-Mass.

The author is grateful is grateful for financial supports by Japan Society of Promotion Science (JSPS). Acknowledgement is also made to all members of Professor Dr. Toshikazu Hirao's group for their hearty supports, encouragement and friendship.

Finally the author would like to express his special gratitude to his parents and family for their constant support, encouragement, and understanding on this work.

Yuki SAKAMOTO